Integrated molecular modelling and machine learning strategies for the design of potential therapeutic agents against Neuroblastoma

By

Mehrosh Agha

Master of Sciences in Bioinformatics

Fall 19-MSBI-NUST00000319400

Supervised by:

Dr. Ishrat Jabeen

Research Center for Modeling and Simulation (RCMS)

National University of Science and Technology (NUST)

Islamabad, Pakistan

December, 2021

Integrated molecular modelling and machine learning strategies for the design of potential therapeutic agents against Neuroblastoma

A thesis submitted in partial fulfilment of the requirement for the degree of Master's in Bioinformatics.

By

Mehrosh Agha

Master of Sciences in Bioinformatics

Fall 19-MSBI-NUST00000319400

Supervised by:

Dr. Ishrat Jabeen

Research Center for Modeling and Simulation (RCMS)

National University of Science and Technology (NUST)

Islamabad, Pakistan

December,2021

Certificate of Originality

I hereby declare that the research work presented in this thesis has been generated by me as a result of my own research work. Moreover, none of its contents are plagiarized or submitted for any kind of assessment or higher degree. I have acknowledged and referenced all the main sources of help in this work.

Mehrosh Agha

Fall 2019-MS BI-4 00000319400

Dedication

I dedicate this work to my beloved Parents for their prayers, love, support, and most of all their huge believe in me and my dreams. Thanks for enlightening me and making me who I am.

Acknowledgment

[*Glory be to You; we have no knowledge except what you have taught us. Verily, it is You, the All-Knower, the All-Wise.* (Surah Baqarah-2:32)]

Allah-there is no deity except Him, the Ever-Living, the Sustainer of [all] existence. We pay our all gratitude to Allah, the Almighty, from whom we seek help, and, in whose premises, there are all lives and matters. We are obligated to Him for all knowledge He has provided us in the completion of this project.

Foremost, I would like to express my sincere gratitude to my advisor Ma'am Ishraat Jabeen for the continuous support of my master study and research, for her patience, motivation, enthusiasm, and immense knowledge. Her guidance helped me in all the time of research and writing of this thesis. I could not have imagined having a better advisor and mentor for my Master Study

Besides my advisor, I would like to thank the rest of my thesis committee: Prof. Dr. Zamir Hussain, Prof. Dr. Tariq Saeed for their encouragement, insightful comments, and hard questions.

I thank my fellow lab mates Syeda Aniqa Bukhari, Rijja Hussain, Aamara Naz Aeman Rauf, Maham Ahmed, for the stimulating discussions, for the sleepless nights we were working together before deadlines, and for all the fun we have had in the last two years.

Last but not the least, I would like to thank my family: my parents Agha Amjadullah Nosheen Naz, for giving birth to me at the first place and supporting me spiritually throughout my life. I would like to Thanks specially my husband Taha Ahmed for supporting me in my studies and decisions. I would like to Thanks my mother in law Kaneez Fiza for taking care of my daughter when I was doing my Master's studies last but not the least I would like to thanks all my brothers and sisters for supporting me and trusting me .

TABLE OF CONTENTS

List of Abbreviations

pNTS	peripheral neuroblastic tumors
INSS	International Neuroblastoma Staging System
DI,	DNA index
FH	favorable histology
UH	unfavorable histology
MYCN	v-myc myelocytomatosis viral related oncogene, neuroblastoma
RynR	ryanodine receptors
InsP3R	inositol triphosphate receptors
CCBs	Calcium channel blocker
cAMP	cyclic adenosine monophosphate
SR	sarcoplasmic reticulum
ER	endoplasmic Reticulum
ALK	Anaplastic Lymphoma Kinase
SF	selectivity filter
GOLD	Genetic Optimization for Ligand Docking
RMSD	Root Mean Square Deviation
SMILE	Simplified Molecular-Input Line-Entry System

List of figures

List of Tables

ABSTRACT

Neuroblastoma is cancer that develops from immature nerve cells found in several areas of the body. It arises from undifferentiated sympathetic-adrenal lineage cells and is mostly intermittent. Intracellular calcium ion concentration is highly maintained in cells as it controls many cellular processes such as ATP synthesis cell cycle apoptosis and much more. Due to the increase of calcium ions, there occurs the disturbance in homeostasis of the calcium apoptosis pathway which leads to neuroblastoma cancer. This rise in Calcium ion due to overexpression of T-type calcium channels in neuroblastoma is our focus of our study.

Overexpression of T type Calcium Channels is because of duplication of gene responsible of encoding T type Calcium Channel i.e., CACNA1G which encode for alpha- pore forming domain of Cav3.1.

The detailed study of T-type calcium channel and its elongation time due to mutation in Cav3.1 (CACNA1G) gene which leads to increase in calcium ion concentration and result to trigger proliferation in neuroblastoma cells instead of apoptosis. We will focus on making calcium channel blockers which mat assist to down-regulate the concentration of T-type channels in neuroblastoma hence leading to a decrease in the level of calcium in cells which will ultimately induce apoptosis in neuroblastoma cells.

Therefore, in this study calcium channels blockers were identified which will help in closing of calcium channel hence maintain the hemostasis of calcium leading to apoptosis instead of cell proliferation. Calcium channel blockers were designed using pharmacophore model s and out of which 8 hits were also identified which can be used as a repurposed drug.

Active site residues like Leu352, Thr353, Glu 354, Ile 380, Ser 383, Phe 384, Asn 952, Tyr 953, Phe 956, Asn 957, Ser 1461, Asn 957, Val 960, Glu 922, Glu 923, Lys 1462, Gln 1816 were identified and seen in molecular docking as well which was verified using PLIF analysis as well. Later on pharmacophore model was built which consists of 9 pharmacophore features out which 2 were hydrogen bond acceptor and 7 were hydrophobic

interactions. This pharmacophore was screened and lastly 8 potential hits were found which can help us block the activity of calcium channel.

CHAPTER 01

INTRODUCTION

Neuroblastoma is most prominent extra cranial solid tumor in children.(1) It is characterized by a neoplastic proliferation of neural crest cells in the evolving sympathetic nervous system. Neuroblastoma is a diverse cancer with predictions ranging from close survival to a high risk of death.(2) Primary tumor can originate somewhere adjacent to the sympathetic system but most commonly it arises in adrenal glands. Differentiation patterns in neuroblastoma tumor cells may help determine patient diagnosis.(3) Most neuroblastomas are made up of embryonic stem cells, some do have fully mature ganglion cells, which are present in ganglioneuromas. The cause of these Sympatico-adrenal lineages' failure is still unclear.(4)

1.1 Epidemiology

The annual occurrence of neuroblastoma in children under the age of 15 is 10.5 per million. Neuroblastoma causes approximately 8% to 10% of all pediatric malignancies and 15% of all cancer mortality in children.(2) According to the American Cancer Society's 2014 pediatric and adolescent cancer statistics, neuroblastoma (7 percent) is the third most common cancer in children, after behind acute lymphocytic leukemia (26 percent) and brain and CNS tumors (21 percent). Neuroblastoma is significantly more common in the United Kingdom, accounting for roughly 8% of all childhood cancers. (3)Neuroblastoma has a pathogenesis that is unknown. With a ratio of 1.2 to 1, it is significantly more common in boys than in females.(5)

1.2 Location of Neuroblastoma

Neuroblastoma can develop in people who have other neural crest abnormalities or cancers. Appearance of neuroblastoma is related with the site of origin of tumor, the extent of spread of disease and paraneoplastic syndromes presence.(6) Majority of neuroblastomic tumor around 65 percent arises in the abdomen. Out of these more than half arises in the adrenal glands. The tumor can also originate in neck, chest, and pelvis. There is a concordance with age and site of disease, with infants more likely to present with thoracic and cervical primary sites. Regional or localized disease is present in almost 50 percent of patients.(7) These patients are usually asymptomatic and this condition is diagnosed with other medical issues. 35 percent of patients have regional lymph node spread at the time of diagnosis accompanied by mass or abdominal distention and pain.(1)

Spread of neuroblastoma occurred through lymphatic and hematogenous routes which include bone, bone marrow, and liver.patients who have wide spread of disease have symptoms which include fever, pain and irritability. children diagnosed with neuroblastoma usually have raccoon eyes i.e. periorbital swelling and ecchymosis.(8)

1.3 Pathology of Neuroblastoma

Neuroblastoma belong to ‘‘small blue round cell’’ neoplasms of childhood. They are also called as the peripheral neuroblastic tumors (pNTs). They are derived the sympathogonia of the sympathoadrenal Lineage which are the progenitor cells of the sympathetic nervous system.(9) After the migration of these immature sympathogonia cells they form the sympathetic ganglia, the chromaffin cells of the adrenal medulla, and the paraganglia, which are the typical areas of neuroblastoma cancer.(10)

The mechanisms causing embryonal cells perseverance that later give rise to pNTs are mainly unknown. One of the major cause of this can be defect in genes controlling neural crest development in embryonic stages. This lead to unbalanced proliferation and improper differentiation of neuroblastoma.(11) These genetic defects causing an unbalanced events of normal genetic differentiation program. The typical pNT subtypes of neuroblastoma have a larger range of maturation, ranging from tumours with predominantly undeveloped neuroblasts to those with a thick stroma of Schwann cells. Cellular heterogeneity is one of neuroblastoma's most distinguishing features. The reason was phenotypically diverse cells could be ongoing mutagenesis but rare multipotent stem cells with indefinite potential for self-renewal drive the onset and growth of tumors could also be another reason.(3). The Notch, Sonic hedgehog, and Wnt/b-catenin pathways, which drive self-renewal in neural stem cells, have all been linked to embryonic cancer. It is possible that neuroblastoma stem cells develop from normal neural crest stem cells, partially retaining and partially disrupting these pathways.

Stages of Neuroblastoma

The current standards for neuroblastoma diagnosis and staging are based on the International Neuroblastoma Staging System (INSS) procedures, which were first developed in 1986 and updated in 1988. The following table below show the classification

of neuroblastoma according to resectability.(12) Resectability means removal of tumor without removal of any important organ or blood vessels.

Tumors that an been removed permanently by surgery are classified as stage 1 whereas partially removal of regional tumors with or without involvement of lymph nodes are classified into stage 2 and 3. Further stage 2 and 3 are classified on basis of amount of tumor which can be resected, spread of tumor in local areas and the regional node involvement. Stage 4 is defined as heterogeneous spread of disease where spread of cancer cells can be in any organ except liver skin and bone marrow involvement whereas in stage 4S spreading of cancer cells in bone marrow, bone and skin is involved seen in the majority of patients greater than 18 months of age.(13)

Table 1: Stages of neuroblastoma

Stage	Description
Stage 1	In this stage tumor is localized tumor with complete gross excision with or without microscopic residual disease. nodes attached to and removed with the primary tumor may be positive
Stage 2A	In this stage tumor is Localized tumor with incomplete gross resection; ipsilateral non adherent lymph nodes are not present for tumor microscopically
Stage 2B	Localized tumours with or without full gross resection and non - adherent lymph nodes on the same side of the body are tumour positive; larger opposite lymph nodes must be microscopically negative.
Stage 3	Here tumor is Unresectable unilateral tumor sensitive across the midlinea with or without regional lymph node involvement
Stage 4	Any primary tumor with spreading to distant lymph nodes, bone, bone marrow, liver, skin, or other organs (except as defined for stage 4S)
Stage 4S	Localized primary tumor (as defined for stage 1, 2A, or 2B) with spreading limited to skin, liver, or bone marrow (limited to infants <1 yr of age)

1.4 Stages and Age relation in Neuroblastoma

The patient's age is a significant clinical prognostic factor. Patients who have been diagnosed with disseminated illness and are older than 1 to 2 years have a poorer prognosis than those who are younger. The age of 365 days has been regarded as a model for tumor behavior until recently, but other ages have been investigated.(14)

Several factors of clinical and biological factors have been to predict clinical behavior of neuroblastoma. For best prediction of clinical prognosis combination of clinical and biological factors plays an important role which have been agreed internationally (15)

Table 2: Children's Oncology Group divided patients into low-, intermediate-, or high-risk categories based upon age at diagnosis, INSS stage, tumor histopathology, DNA index (ploidy), and MYCN amplification status, with each group displaying a unique risk for recurrence

			MYCN Amplification		
Risk Group	Stage	Age	Status	Ploidy	Shimada
Low risk 1	1	Any	Any	Any	Any
Low risk	2a/2b	Any	Not amplified	Any	Any
High risk	2a/2b	Any	Amplified	Any	Any
Intermediate risk	3	<547 d	Not amplified	Any	Any
Intermediate risk	3	>= 547 d	Not Amplified	Any	FH
High Risk	3	Any	Amplified	Any	Any
High risk	3	>=547d	Not Amplified	Any	UH
High Risk	4	< 365 d	Amplified	Any	Any
Intermediate Risk	4	< 365 d	Not Amplified	Any	Any
High risk	4	365 to < 547 d	Amplified	Any	Any
High risk	4	365 to < 547 d	Any	DI=1	Any
High Risk	4	365 to < 547 d	ANY	Any	UH
Intermediate Risk	4	365 to < 547 d	Not Amplified	DI>4	FH
High risk	4	>=547 d	Any	Any	Any
Low risk	4s	< 365 d	Not Amplified	DI>4	FH
Intermediate risk	4s	< 365 d	Not Amplified	Di=1	Any
Intermediate risk	4s	< 365 d	Not Amplified	Any	UH
High risk	4s	< 365 d	Amplified	ANY	Any

1.5 Cause of Neuroblastoma

There are several causes of neuroblastoma out of which one is genetic cause and other is disruption in calcium ion hemostasis leading to disruption in cell cycle and causing neuroblastoma.

1.5.1 Genetic Cause

Neuroblastoma are divided into two classes. Almost 45 percent of neuroblastomas are near-diploid nuclear DNA content and 55 percent are Near-triploid neuroblastomas consists of whole chromosome gains and losses without structural genetic aberrations. In clinical studies Clinically localized tumors are mostly, near-triploid tumors are more often and show a favorable outcome.(16) The presence of genetic aberrations, such as MYCN amplification, 17q gain, and chromosomal losses are present in Near-diploid neuroblastomas. (17). One of the most common chromosomal alterations in neuroblastoma is the deletion of a portion of chromosome 1p, which is linked to a poor prognosis. In a study, multivariate analysis showed that deletion of chromosome 1p was a major prognostic factor in a study evaluating cytogenetic variables in 89 neuroblastomas. Patients with stage 1, 2, or 4S illness had a better three-year event-free survival rate than those with chromosome 1p allelic deletion. (18) Overexpression and amplification (increased copy number) of oncogene MYCN, a close relative of the oncogene c-myc that resides on chromosome 2p, is highly associated with deletions of 1p. persistent high levels of the MYCN protein occurs because of Gene overexpression.(19) MYCN Protein is a DNA binding transcription factor responsible for malignant alteration in both in vitro and in vivo tumor models. . A 50- to 400-fold amplification of MYCN is found in approximately 25 percent of neuroblastomas and is an indicator of poor prognosis.(20)

Patients with MYCN amplification have poor prognosis and overall survival rate is also low i.e. 72 versus 98 percent compared with patients having no MYCN amplification. The absence of MYCN amplification and the absence of other structural abnormalities, such as in 11q or 17q, can define low-risk tumors.(21) Deletions of 11q and/or 14q are detected in 25 to 50 percent of neuroblastomas. Neuroblastomas that are characterized by these changes generally lack 1p deletions and MYCN amplification, and they appear to represent a distinct tumor subtype. A gain of chromosome 17q material (trisomy 17q) occurs in over

one-half of neuroblastoma and appears to be associated with a particularly aggressive phenotype.

In additional to structural chromosomal changes, alterations in total DNA content, which presumably result from mitotic dysfunction, are an important indicator of both outcome and response to therapy. Neuroblastomas with a higher DNA content (hyperdiploid, with a DNA index [DI] >1) are associated with lower tumor stage, better response to initial therapy, and an overall better prognosis than diploid tumors (ie, DI = 1), particularly if they lack MYCN amplification(15)

1.5.2 Role of Calcium in neuroblastoma

Calcium is an important signal messenger element involved in the regulating many cellular functions including cell cycle. Maintenance of hemostasis of of intracellular Calcium ionis important for the cell cycle .Excessive calcium or loss of control in calcium signaling can lead to cell death and result in cell proliferation i.e. tumor. .(20) As a result, calcium signalling regulation is necessary for cell survival. Calcium can be released from intracellular reserves or influxed through a variety of plasma membrane ion channels, resulting in an increase in cytoplasmic calcium. Calcium ionfluxes to the cytoplasm are provided via voltage-gated and ligand-gated Calcium ionchannels in the plasma membrane, along with ryanodine receptors (RynR) and inositol triphosphate receptors (InsP3R) at intracellular calcium reserves. The driving force for calcium entry is the result of an electrochemical gradient between the extracellular concentration (1.3 × 10-3-2 × 10-3 mol/L) of calcium and the intracellular concentration (< 10-8 mol/L).(22) When calcium is transported in mitochondria it activates apoptosomes which further

activates caspases and hence leading to apoptosis in a normal calcium regulation.

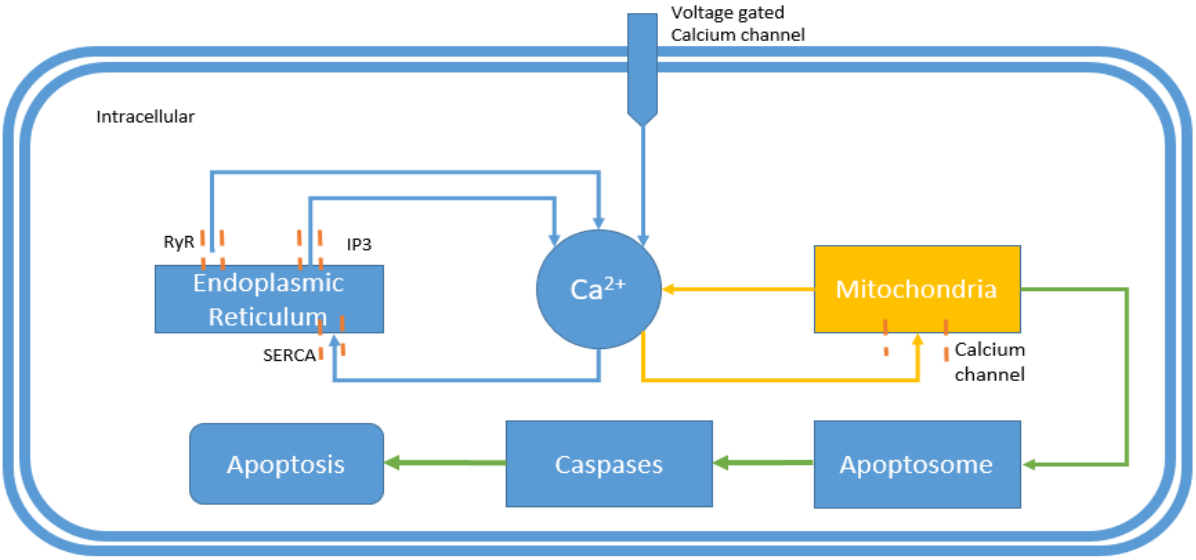

Figure 1: Flow of calcium in normal cell

Whereas in cancerous cell when there is overexpression of voltage gated calcium channels, there is influx of more calcium and as a result increase in intracellular calcium ion leads to more influx in mitochondria.(23) When there is signal of abundant calcium ion it activates the TCA cycle for growth as the formation of ATP is abnormally high and consistent calcium ions due to over expression of voltage gated calcium channels lead to the abnormality and hence abnormal growth leading to neuroblastoma cancer. (24)

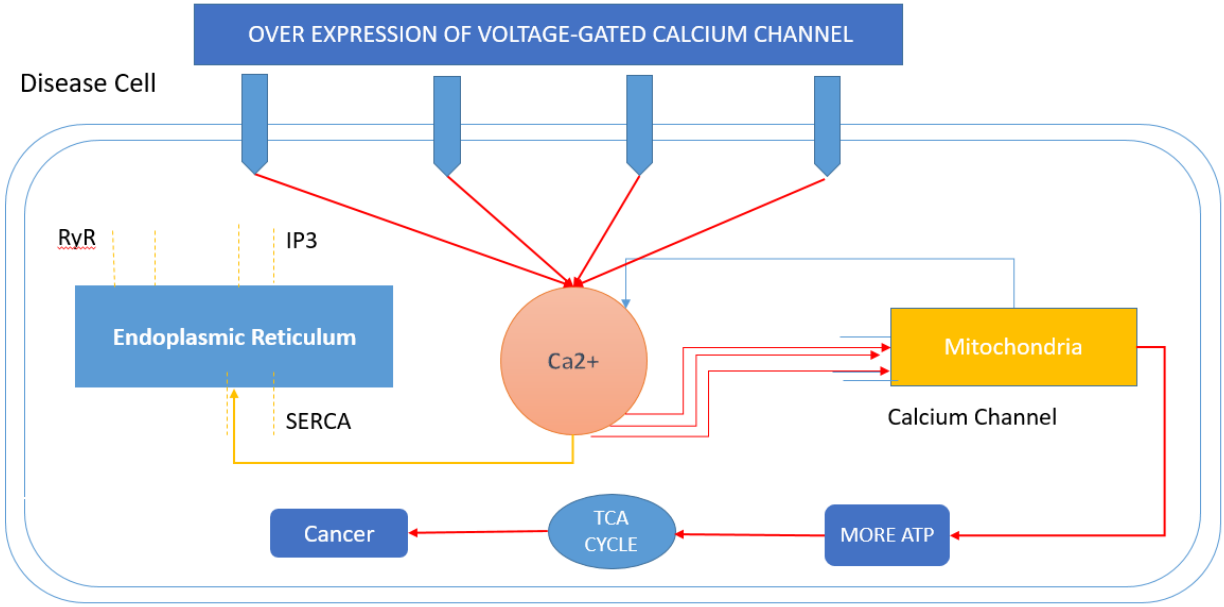

Figure 2: Flow of calcium in disease cell

1.6 Calcium Channel

Calcium channels serve as a key transducers of cell surface membrane potential changes into local intracellular Calcium iontransients that is responsible for introduction of many cell events. In many distinct cell types, voltage-gated Calcium ionchannels govern intracellular activities such as contraction, secretion, neurotransmission, and gene expression by mediating Calcium ioninflow in response to membrane depolarization. (25)Their presence is required to link electrical signals on the cell surface to physiological processes within cells. They belong to the transmembrane ion channel protein gene superfamily, which also contains voltage-gated potassium and sodium channels. and γ. Of these, the alpha1 subunit comprises the pores of the calcium channel and the binding sites for CCBs.(26) With four major domains, each with six transmembrane units, the subunits have a complex structure. Between the fifth and sixth units, calcium channel pores occur, and the voltage sensor is located near each domain's fourth transmembrane device.(27)

Two regulatory aspects of the blockade of calcium channels are essential. First, when cyclic adenosine monophosphate (cAMP) activates protein kinase A to phosphorylate the calcium channel, the COOH-terminal portion of each of the alpha1 subunits has several phosphorylation sites available. Such phosphorylation allows a more open state of the

channel to persist. Second, the β subunit binds to the cytoplasmic link of the γ1 subunit between domains I and II and thus increases the opening of the calcium channel.

There are three types of calcium channels but our channel of interest discussed here in T type calcium channel.

1.6.1 T-type Calcium Channel

T-type calcium channels are low-voltage activated calcium channels that become inactivated during excitability of the cell membrane but reactivate during depolarization. The entry of calcium into various cells triggers a variety of physiological reactions. The activation of the voltage-gated calcium channel in cardiac muscle cells and smooth muscle cells causes a rise in cytosolic level, which causes contraction[28]. T-type calcium channels are not only considered to be found within the cardiac and smooth muscle but are also present within the central nervous system in many neuronal cells.[29] The separation of T-type calcium channels (transient opening calcium channels) from the already well-known L-type calcium channels was made possible by numerous experimental experiments in the 1970s (Long-Lasting calcium channels).(28)

Due to their ability to be activated by more harmful membrane potentials, the new T-type channels were substantially different from the L-type calcium channels, had limited single-channel conductance, and were also not immune to calcium antagonist drugs that were present. The cortex, peripheral nervous system, heart, smooth muscle, bone, and endocrine system are normally found inside these different calcium channel(20)

In additional to structural chromosomal changes, alterations in total DNA content, which presumably result from mitotic dysfunction, are an important indicator of both outcome and response to therapy. Neuroblastomas with a higher DNA content (hyperdiploid, with a DNA index [DI] >1) are associated with lower tumor stage, better response to initial therapy, and an overall better prognosis than diploid tumors (ie, DI = 1), particularly if they lack MYCN amplification(15)

1.6.2 Role of Calcium in neuroblastoma

Calcium is a signal transduction element that regulates numerous eukaryotic cellular activities, including cell cycle progression. Control of intracellular Calcium ionis critical for the cell cycle and plays an important role in the regulation of cell proliferation and

growth; however, too much calcium or a lack of control over calcium signaling can lead to cell death..(20) As a result, controlling calcium signalling is essential for cell survival. Increased cytoplasmic calcium can be caused by either intracellular calcium release or influx through a number of plasma membrane ion channels. Calcium ion fluxes to the cytoplasm are provided via voltage-gated and ligand-gated Calcium ion channels in the plasma membrane, as well as ryanodine receptors (RynR) and inositol triphosphate receptors (InsP3R) at intracellular calcium reserves The driving factor for calcium entry is caused by a concentration gradients between the extracellular concentration of calcium (1.3 10-3-2 10-3 mol/L) and the intracellular concentration (10-8 mol/L). [21] When calcium enters mitochondria, it triggers apoptosomes, which then activate caspases, resulting in apoptosis in a normal calcium regulation.

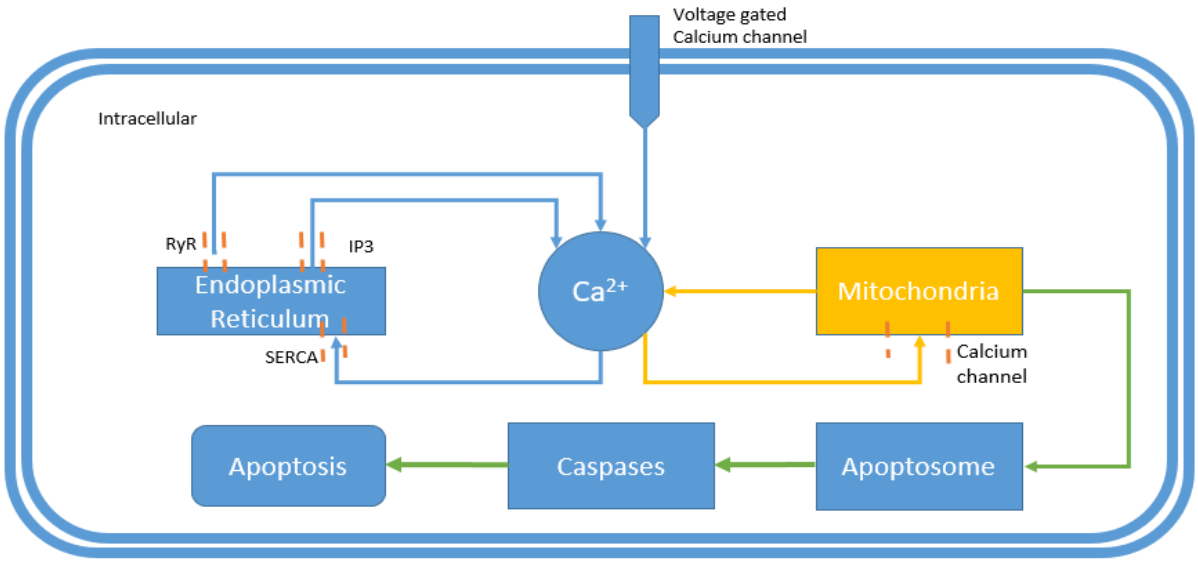

Figure 1: Flow of calcium in normal cell

Whereas in cancerous cell when there is overexpression of voltage gated calcium channels, there is influx of more calcium and as a result increase in intracellular calcium ion leads to more influx in mitochondria.(23) When there is signal of abundant calcium ion it activates the TCA cycle for growth as the formation of ATP is abnormally high and consistent calcium ions due to over expression of voltage gated calcium channels lead to the abnormality and hence abnormal growth leading to neuroblastoma cancer. (24)

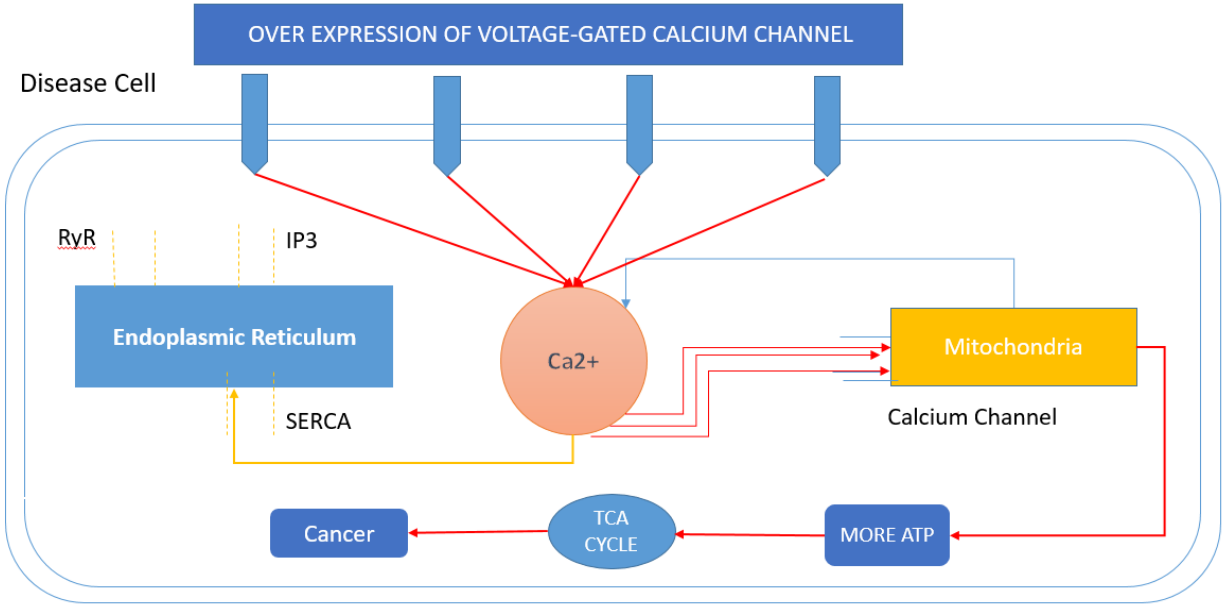

Figure 2: Flow of calcium in disease cell

1.7 Calcium Channel

Calcium channels serve as a key transducers of cell surface membrane potential changes into local intracellular Calcium iontransients that is responsible for introduction of many cell events. In many distinct cell types, voltage-gated Calcium ionchannels govern intracellular activities such as contraction, secretion, neurotransmission, and gene expression by mediating Calcium ioninflow in response to membrane depolarization. (25)Their presence is required to link electrical signals on the cell surface to physiological processes within cells. They belong to the transmembrane ion channel protein gene superfamily, which also contains voltage-gated potassium and sodium channels. and γ. Of these, the alpha1 subunit comprises the pores of the calcium channel and the binding sites for CCBs. With four major domains, each with six transmembrane units, the subunits have a complex structure. Between the fifth and sixth units, calcium channel pores occur, and the voltage sensor is located near each domain's fourth transmembrane device.(27)

Two regulatory aspects of the blockade of calcium channels are essential. First, when cyclic adenosine monophosphate (cAMP) activates protein kinase A to phosphorylate the calcium channel, the COOH-terminal portion of each of the alpha1 subunits has several phosphorylation sites available. Such phosphorylation allows a more open state of the

channel to persist. Second, the β subunit binds to the cytoplasmic link of the γ1 subunit between domains I and II and thus increases the opening of the calcium channel.

There are three types of calcium channels, but our channel of interest discussed here in T type calcium channel.

1.7.1 Structure of T-type calcium channel

T type calcium channels, like high-threshold calcium and sodium channels (56, 57), are made up of four homologous repetitions (I–IV), each with six transmembrane segments (S1–S6), containing a highly conserved pore loop (between S5 and S6) and a separate voltage sensor (between S5 and S6) (S4). The extensive intracellular loops, notably the one connecting domains II and III, which also contains a site for alternative splicing in alpha1G, show greater variation between isoform sequences.(29) This conformational change of the channel is responsible for the interaction of several calcium channels with specific cell proteins [such as the ryanodine receptor binding to the skeletal muscle L-type channel, or syntaxin binding to the neuronal N-type channel, and could thus contribute to the formation of specific functions for each channel isoform within the cell] and could thus play a role in the formation of specific functions for each channel isoform inside the cell.(30)

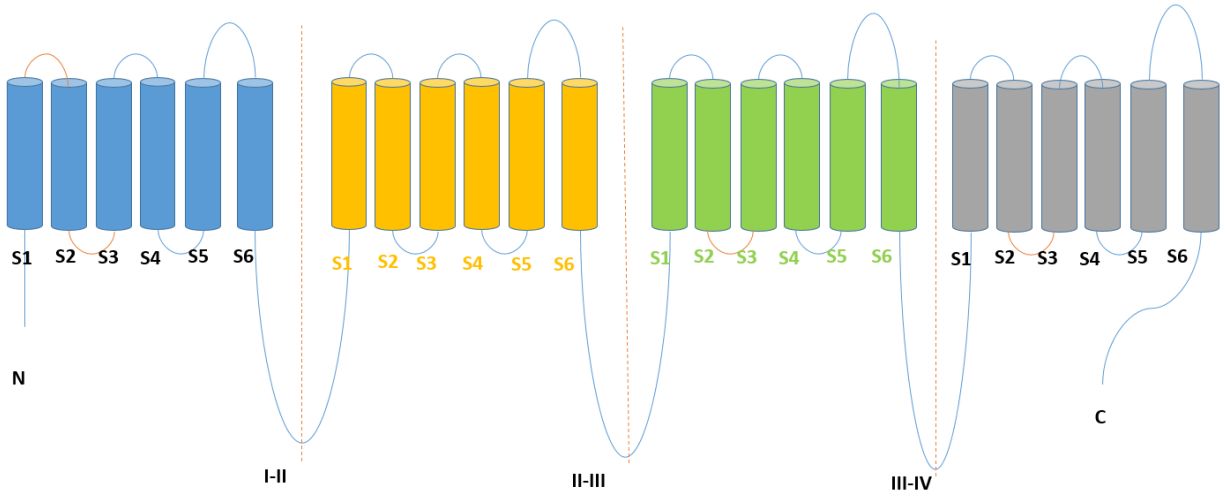

Figure 3: Structure of Calcium channel Alpha-1 subunit

1.8 Challenges

The main challenge in our study is tissue specificity of Cav3.1. Cav3.1 is highly expressed in brain, in the amygdala, sub thalamic nuclei, cerebellum and thalamus. Moderate expression in heart; low expression in placenta, kidney and lung. Also expressed in colon and bone marrow and in tumoral cells to a lesser extent. Highly expressed in fetal brain, but also in peripheral fetal tissues as heart, kidney and lung, suggesting a developmentally regulated expression

Introduction of our drug without any toxicity introduction in body which is main challenge of our study due to expression of calcium channel in tissue.

1.9 Problem statement

There are two main organelles responsible for regulation of calcium ions in cells Endoplasmic Reticulum and Mitochondria. Endoplasmic Reticulum serves as a storage for Calcium whereas mitochondria use calcium for energy production via TCA cycle. When there is excess of calcium because of over expression of calcium channels, instead of apoptosis cell will begin to grow because f more ATP production hence leading to neuroblastoma i.e. cancer cell proliferation

1.10 Proposed strategy

There is a need for designing calcium blockers which will block the calcium channels and so no extra calcium will be present in cell for mitochondria to show irregular TCA cycle.

1.11 Objectives

- To identify various predictive models for the modulators of T-type calcium ion channels
- To Develop models for classification and identification of ligand data set using Machine learning models
- To develop an in-silico protocol for the identification of potential modulators of T-type calcium ion channels for the modulation of neuroblastoma

CHAPTER 02

LITERATURE REVIEW

2.1 Cell cycle stages and calcium role

The cell cycle has four stages: G1, S, G2, and M. The S phase is responsible for DNA replication, while the M phase is responsible for mitosis. Cells must pass through a restriction barrier between the G1 and S phases before they may continue to proliferate; otherwise, they leave the cell cycle at G0 and either differentiate or die. Another cell cycle checkpoint occurs between phases G2 and M. Calcium ionis one of the most important transmitters for cells to cross via these numerous locations.$^{+\cdot}$(31)

Steinhardt et al detected transitory increases in cytosolic Calcium ionat late G1, before to the start of the S phase, and during G2 before the start of the M phase, which were dependent on external Calcium ionconcentration. Cells require external Calcium ionin addition to operational calcium channels to activate a slew of critical downstream enzymes directly or indirectly such as thymidine kinase, thymidylate synthase, ribonucleotide reductase, and DNA polymerase and initiate DNA replication during the transition from G1 to S phase. Calcium ionflashes stimulate enzymes required for microtubule reorganization and microfilament contraction during the shift from G2 to M phase. (32). Pharmacological investigations utilising Calcium ionchannel antagonists clearly illustrate the role of Calcium ionchannels on cell development. Cells can commit suicide at the conclusion of the cycle by a process known as apoptosis or active cell death, which is a genetic program particularly intended to form organs during development and modify cell population levels to acceptable values [31]. A deadly Calcium ionsurge and the nuclear membrane Calcium iontriggered endonuclease, which ends the cell by breaking chromatin into pieces, are the major actors in apoptosis. Underlying mechanisms for Calcium ionmediated effects in cell proliferation may involve a wide variety of other intracellular signal transduction pathways such as G-proteins, protein kinase C (PKC), calmodulin, m-calpain, MAP kinase, phospholipase A2 and others. (33).

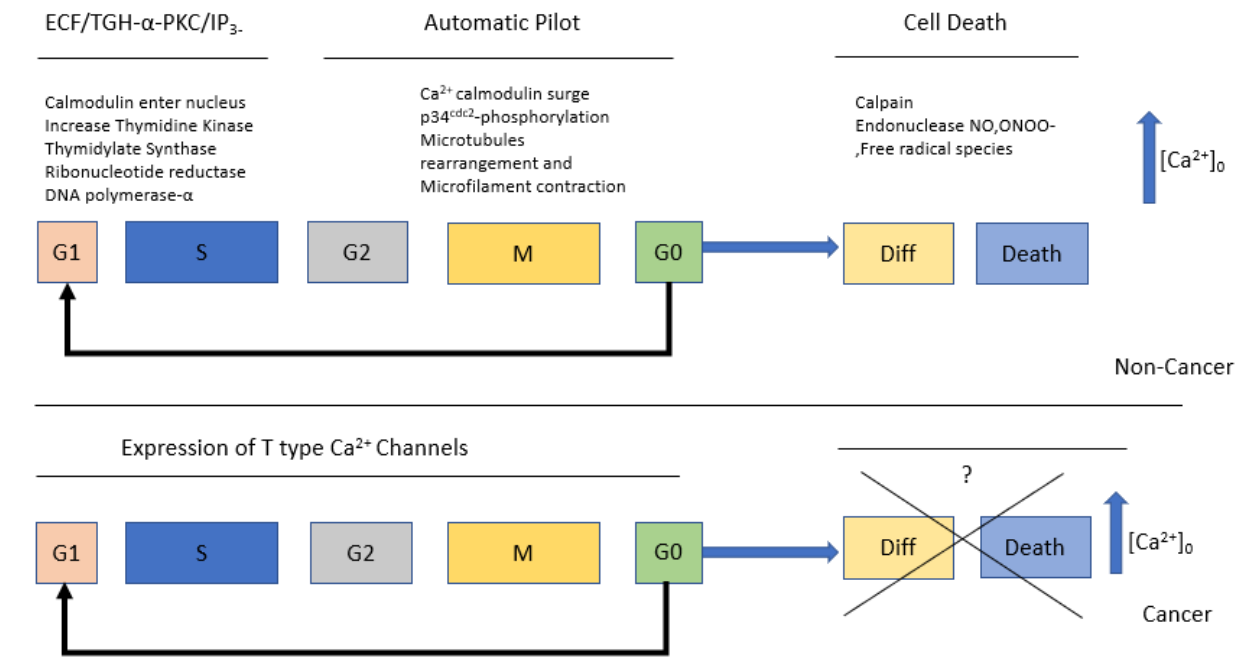

Figure 4: Calcium ionsignaling pathways differ between tumor and normal cells

One method is the breakdown of inositol lipids by the enzyme phospholipase C, whose activation is reliant on an initial increase in Calcium ion and results in the formation of triacylglycerol (DAG) and InsP3. InsP3 triggers Calcium ion dependent Calcium ion release from intracellular storage as a result of activation of G protein-linked or tyrosine-kinase-linked receptors. (33) This Calcium ion release, described as "calcium puffs" that spread into a local or global Calcium ion signal, is critical for transforming the cytoplasm into an excitable medium capable of supporting recurrent Calcium ion oscillations (34). The resulting amplification of Calcium ion contributes to the signal for mitosis and DNA synthesis.

Sensory proteins, in addition to InsP3, play a function in the calcium signaling system's maintenance. Calmodulin is a calcium-binding protein that functions as a Calcium ion sensor during the cell cycle. (35) Calmodulin is expressed at high levels during the S phase during mitosis, and blocking its action with calmodulin monoclonal antibodies has been demonstrated to stop DNA synthesis.(36)

2.2 Role of calcium channel in cancerous cell cycle

During cell cycle, calcium signaling in malignant cells employs a different mechanism. Calcium ion signal spikes are ineffective in terminating mutant cells because the cells are no longer sensitive to Calcium ion signals; instead, they generate and react to their own renegade growth factors.(30)Calcium ion and Ca^{2+}-binding proteins, as well as the signaling enzymes that are directly triggered by Calcium ion or by Ca^{2+}-binding proteins, play critical roles in most cell signals and program, and must be understood and integrated in any future differentiation therapies. T-type Calcium ion channels are expressed in malignant cells, thus it's probable that these channels provide a different Calcium ion influx mechanism in response to the increased demand for Calcium ion during fast cell growth.

To avoid functional production of the protein if these channels do engage in proliferation under aberrant circumstances, cells must first retain control of the expression of 1G T-type Calcium ion channel messenger RNA. If this regulation is lost, it can lead to abnormal cell proliferation and tumor development.

Table 3: Cancerous cells that express T-type Calcium ionchannels

Cell type	Cell line	T-type isoform
Breast Carcinoma	MCF-7, MDA-435 MDA-231, MDA-361 MB-468, MB-474, BT-20, CAMA1, SKBR-3	α1G, α1H α1G
Neuroblastoma	SK-N-SH, NG 108-15, SK-N-MC	 α1G
Breast carcinoma	MCF-7, MDA-435 MDA-231, MDA-361 MB-468, MB-474, BT-20, CAMA1, SKBR-3 N1E-115	α1G, α1H α1G α1G, α1H
Retinoblastoma	Y-79, WERI-Rb1	α1G, α1H, α1I
Glioma Primary (biopsy)	U87-MG	α1G α1G, α1H
Prostate carcinoma	TSU-PRL, DUPRO LNCaP PC-3, DU-145	α1G α1H α1G, α1H
Esophageal carcinoma	TE1, TE10, TE12, KYSE150, KYSE180, KYSE450	α1H

	SKGT4, TE3, TE7, KYSE70	α1G, α1H
	COLO-680N, SEG1, TE8, TE11, KYSE30, KYSE410, KYSE510	α1G, α1H, α1I
Fibro sarcoma	HT1080	α1G
Colorectal carcinoma	Caco2, DLD-1, Lovo, SW837	α1G
Pheochromocytoma	MPC 9/3L	α1G

2.3 Regulation and signaling of Calcium

Cell fate is influenced by the spatial, magnitude, and temporal features of Calcium ion. In resting cells, Calcium ion entry from the extracellular space or release from internal Calcium ion reserves can result in a 100-fold rise in Calcium ion concentration.(17) To maintain a low Calcium ion level and ensure strictly outlined Calcium ion signals, calcium entry and outflow processes are strictly controlled.(37). Because Calcium ion is plentiful in both the extracellular and intracellular calcium stores, Calcium ion entrance (from the extracellular compartment) or release (from the stores) will elevate the cytosolic Calcium ion-concentration. Calcium ion is lowered by active transport systems, which transfer cytosolic calcium back to storage (Endoplasmic Reticulum (ER) and mitochondria) or into the extracellular space .(38) The systems that regulate Calcium ion, including as Na+/Ca2+-exchangers, calcium pumps, and calcium channels, are changed in cancer.

In muscle cells, the internal reserves of calcium include the endoplasmic reticulum (ER) or a related organelle known as the sarcoplasmic reticulum (SR), where calcium release is primarily regulated by the inositol-1,4,5 triphosphate receptor (InsP3R) and the ryanodine receptor (RYR). The binding of InsP3 and cyclic ADP ribose (cADPR) to the InsP3R and RYR, respectively, releases calcium from the ER. (39). When hormones, growth factors, and the neurotransmitter acetylcholine attach to their cell surface receptors, phosphatidyl inositol 4,5-bisphosphate, a phospholipid present in the cell membrane, is cleaved, InsP3 is produced. Furthermore, the nicotinic acid dinucleotide phosphate (NAADP) and sphingosine-1 phosphate (S1P) release Calcium ionfrom the ER to the NAADP receptor and sphingolipid calcium release-mediating protein. (38).

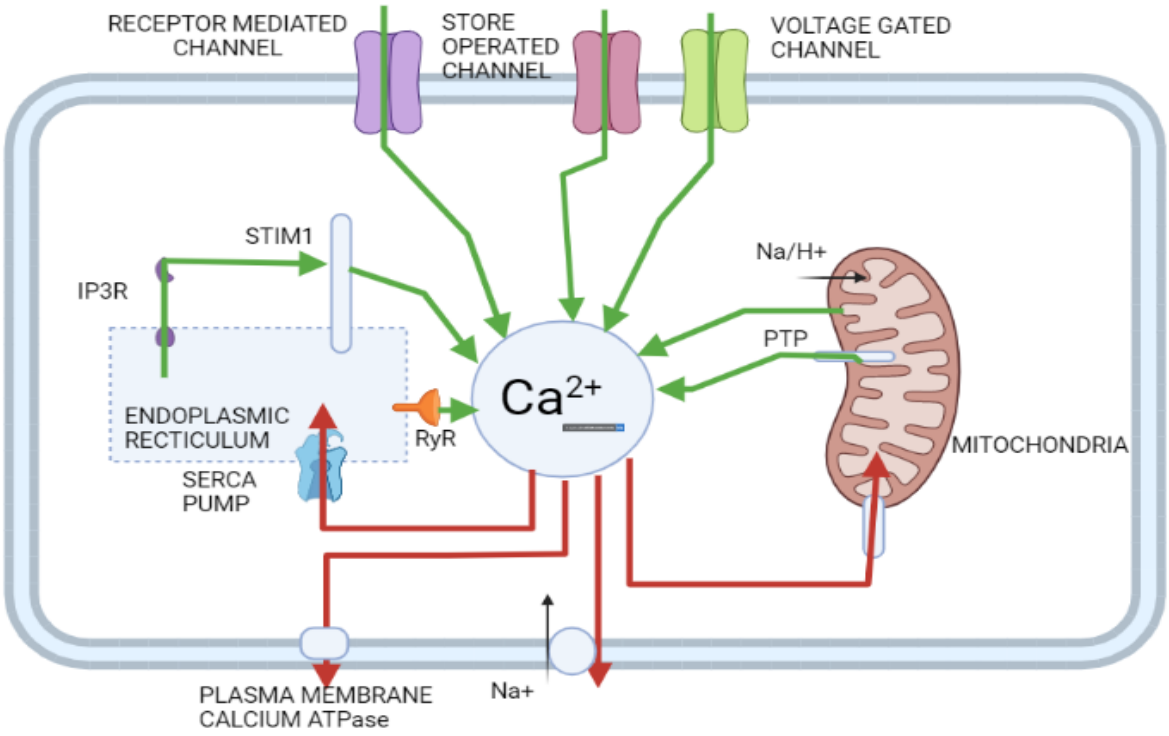

Figure 5: Flow of calcium from in stores organelles and in extracellular environment of cell

Unbalanced cell survival and apoptotic pathways are responsible for neuroblastoma development and malignancy. In neuroblastoma, intracellular calcium stimulates intermediary proteins in signaling pathways.(40). Calcium regulates three kinases involved in cell survival signalling in neuroblastoma (AKT, ERK, and FAK). The intracellular calcium and PI3K/AKT pathways interact, establishing a loop, whereas its influence on the other two kinases is mostly through calmodulin activation and CaM-dependent protein kinase kinases. PI3K/AKT is particularly important since it is a key route in neuroblastoma development that has been identified in primary neuroblastoma cells and other cell lines (including SH-SY5Y, SK-N-SH, SK-N-BE, SK-N-EP and IMR32) [34,35]. By activating survival-associated proteins and blocking the apoptotic pathway, PI3K/AKT increases cell survival. .(40)Several studies looked at how downregulating the PI3K/AKT pathway might increase apoptosis in neuroblastoma cells, and showed that cells with MYCN amplification had more inhibition of the PI3K/AKT pathway, which is thought to be a crucial component in neuroblastoma prognosis .(41)

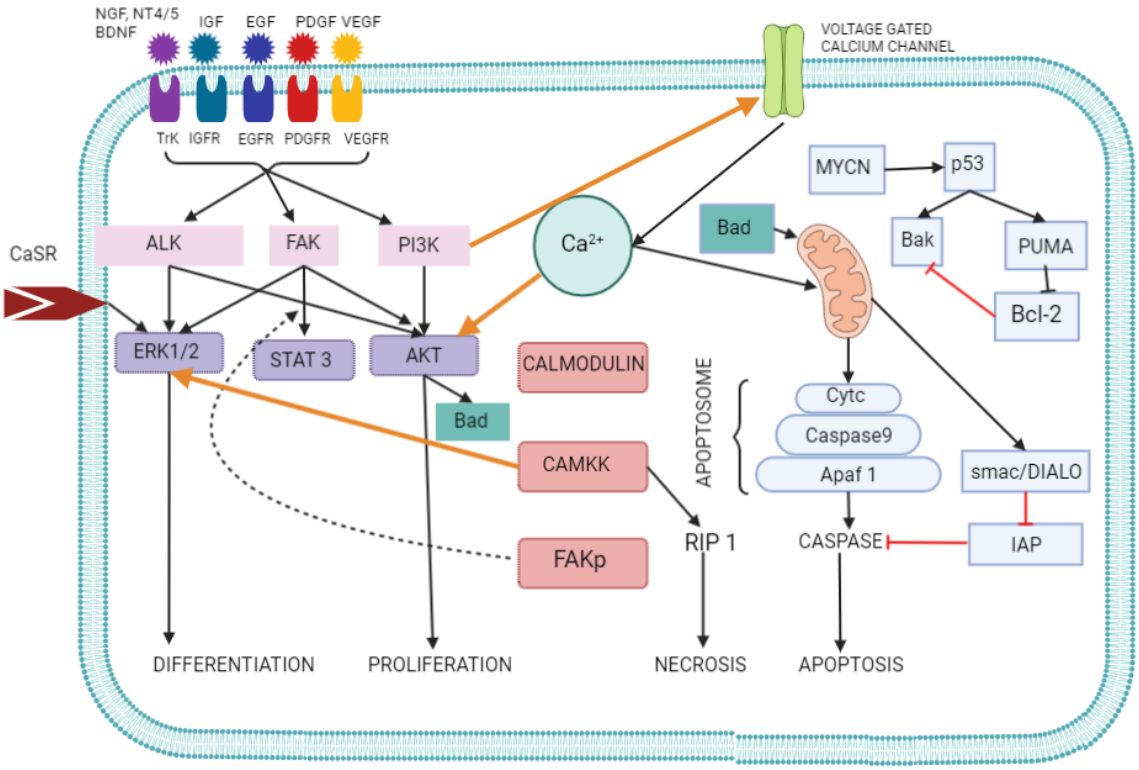

Figure 6: Signaling pathways involving calcium ion responsible for certain processes

Anaplastic Lymphoma Kinase (ALK) is also linked to neuroblastoma cell survival signaling. It is a member of the insulin receptor family that includes the trans-membrane receptor tyrosine kinase and regulates cell growth and development mostly through the central nervous system.(26) ALK protein expression was found in approximately 90% of neuroblastoma tumor samples, and it was linked to ALK gene alterations. Neuroblastoma is linked to ALK gene mutations in both familial and sporadic cases. AKT, ERK1/2, and STAT3 are part of the downstream signaling cascade of ALK signaling. (16). Calcium phosphorylates three kinases (AKT, ERK and FAK) that are involved in the cell survival signaling in neuroblastoma(42)

Because the spontaneous shrinkage of neuroblastoma is done in part by neuronal differentiation of the cells, neuroblastoma is linked to a halt in cell differentiation. Inducing differentiation as a treatment is believed to be one of the most effective therapeutic procedures. In neuroblastoma cell lines, retinoic acid causes differentiation. (43). Patients with high-risk neuroblastoma are now treated with retinoic acid, which inhibits cell growth

and induces differentiation. (44). An increase in Calcium ion is linked to the induction of differentiation in neuroblastoma cell lines.

Neuroblastoma tumors and neuroblastoma cell lines are made up of multipotent progenitor cells that develop into distinct neural crest cell lineages.(45) Neuroplastic N-type cells, substrate adherent S-type cells, and intermediate I-type cells are the three primary cellular phenotypes seen in neuroblastoma cell lines. N-type cells are precursors to the sympatho-adrenal cell lineage and are made up of immature nerve cells. S-type cells are progenitor cells of the neural crest's Schwann, glial, and melanocytic cells and belong to the non-neuronal lineage. I-type cells are intermediate between N- and S-type cells in terms of morphological traits and biological markers., I-type cells are either stem cells or an intermediate stage between N- and S-type cells in the trans-differentiation process. N-type cells are more cancerous, whereas S-type cells are non-cancerous.(26)

2.4. Structural Analysis of Calcium Channel CACNA1G

The Cav3 channels have only about 20% sequence identity and 45 percent similarity to the other two subfamilies. Human Cav3.1, the first Cav channel to be cloned, was discovered 12 years after rabbit Cav1.1, the first Cav channel to be discovered. Variations in the sequence occur throughout the whole sequence, including the selectivity filter (SF). While Cav1 and Cav2 members both feature four Glu residues (EEEE) that determine Calcium ion selectivity (one on the corresponding locus of each repeat), the equivalent loci in the last two repeats are substituted by Asp in Cav3 channels (EEDD). Furthermore, analysis of recombinant generated channels suggests that Cav3 core subunits can operate alone, but the other families require auxiliary subunits for appropriate membrane localization and activity regulation.(46)

Overall structure of human Cav3.1-Δ8b. The four repeats I–IV are colored by domain. Two potential Calcium ions in the selectivity filter (SF) are shown as red spheres. respectively. The disulfide bond between Cys104 and Cys889 is unique to T-type VGCCs shown in pink color in figure below.

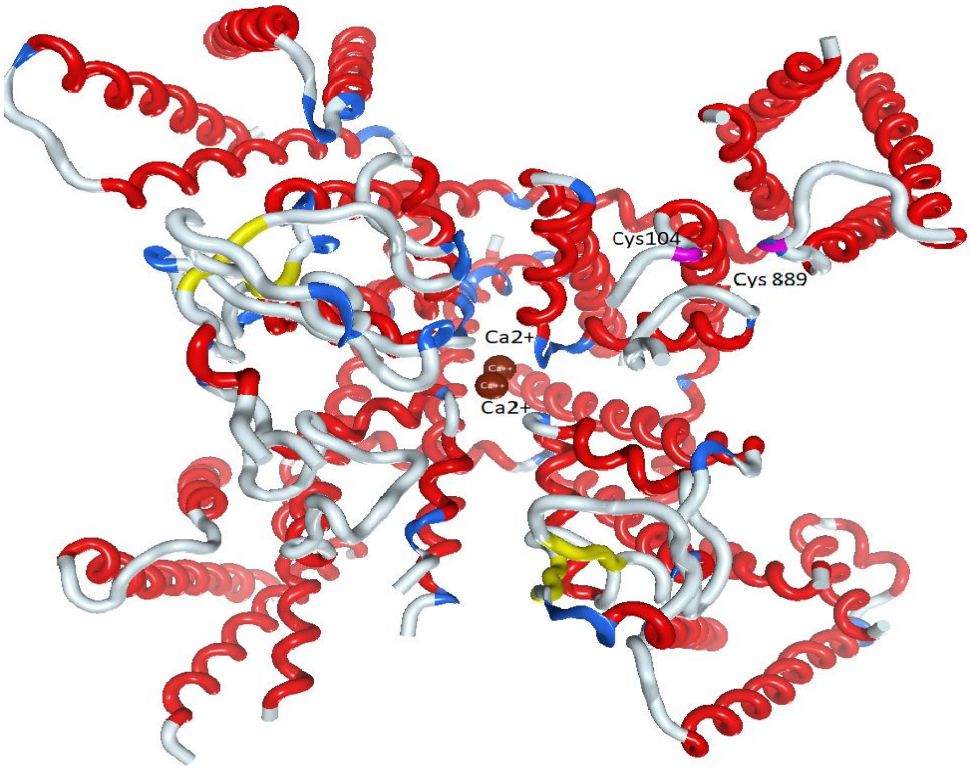

Figure 7: X-ray Crystallographic structure of calcium channel CACNA1G PDB ID: 1KZP

CHAPTER 03

METHODOLOGY

In the current project various pharmacoinformatic including homology molecular docking, pharmacophore modeling and machine learning approaches were applied to probe the 2D and 3D structural features of Calcium channel blockers. Inclusively, a complete workflow of the overall methodology is demonstrated in Figure 8.

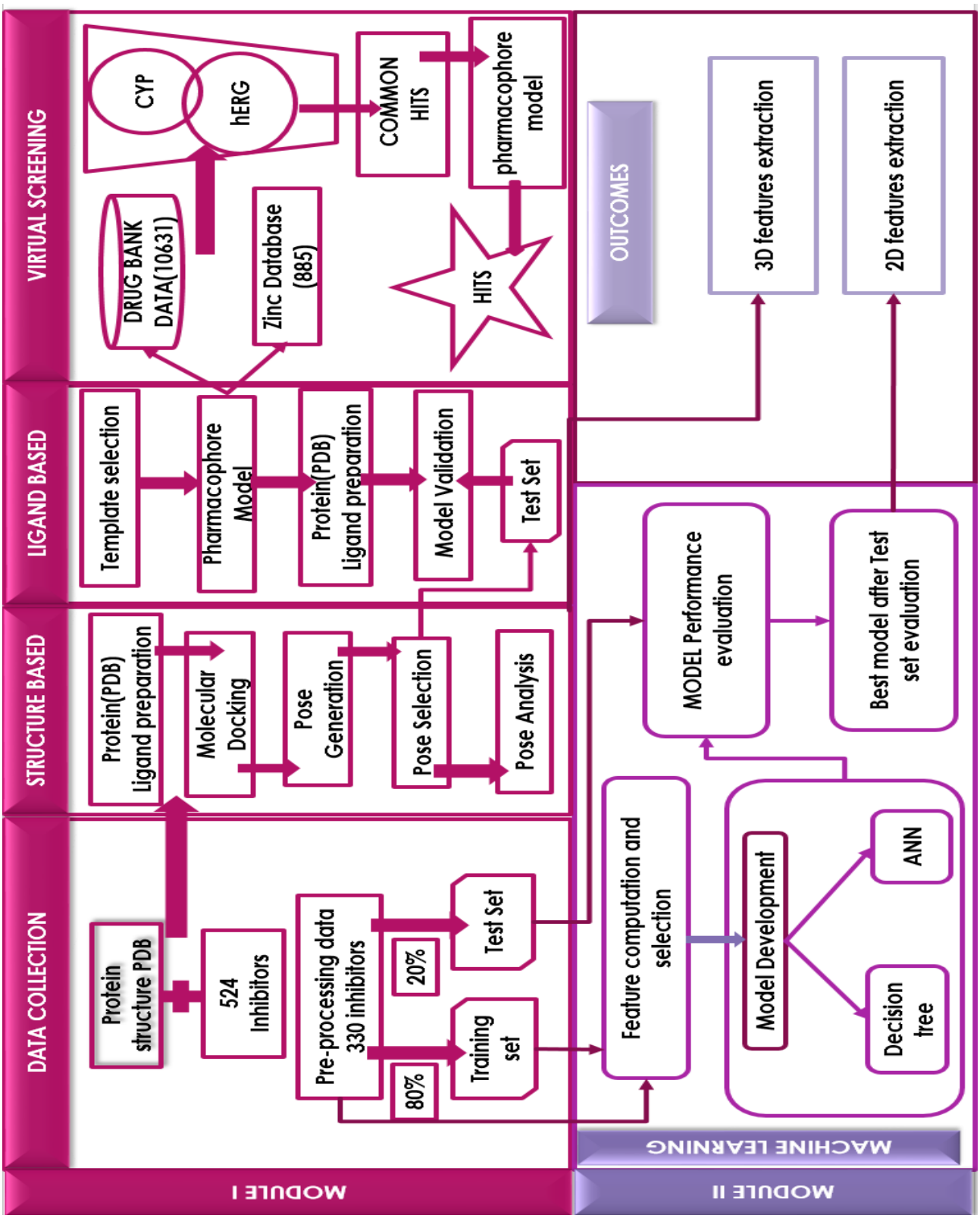

Figure 8: Overall work flow of Methodology

3 Data collection

3.1. Chemical Data Collection

A structurally varied collection of 524 calcium channel CNAC1G ligands was collected from literature and chemical databases (CHEMBL and PubChem), along with their biological activity (IC_{50}) values. Duplicates, racemic compounds, and fragments were then eliminated. Furthermore, molecules with molecular weights less than 200 were omitted from the data since they represent molecular fragments. Following preprocessing, a dataset of 330 ligands was obtained, and the inhibitors dataset was split into two activity levels: active and inactive. Actives were defined as compounds with an IC_{50} value less than 1000nM whilst inactive were compounds with an activity value greater or equal to 1000nM.

3.2. Physiochemical parameters calculation

The descriptors, which are the distinguishing characteristics of molecular structures, represent the properties of a molecular structure. Using the MOE program(47) all 2D descriptors were computed for the whole dataset to investigate how these descriptors affected biological activity. In order to measure the activity of these inhibitors, pIC_{50} was also computed. pIC_{50} is the negative log of the IC_{50} value when converted to molar and aids in understanding activity values.

3.3 Biological Data collection

The X-ray crystallographic structure of Calcium channel CACNA1G (PDB ID: 6KZP) (10.2210/pdb6kzp/pdb) was downloaded from Protein Data Bank (PDB) (https://www.rcsb.org/) and used as a receptor for molecular docking studies.

3.4 Molecular docking

Using the GOLD suite v.5.3.0, molecular docking was used to find the most likely binding conformations of modulators of specified biological targets. In the molecular docking study, the X-ray crystallographic structure of the calcium channel CACNA1G (PDB ID: 6KZP) was employed. However, the binding site of proteins was chosen using a point selection approach in the 20A region, which contains all of the active residues found in the literature. Residues like Leu352, Thr353, Glu 354, Ile 380, Ser 383, Phe 384, Asn 952, Tyr

953, Phe 956, Asn 957, Ser 1461, Asn 957, Val 960, Glu 922, Glu 923, Lys 1462, Gln 1816 known to be the important residues for predicting probable binding cavity and interaction. The energy of the crystal structure was minimized in MOE (Molecular Operating Environment) using the AMBER99 force field. Docking simulations were run using the GOLD suite (Genetic Optimization for Ligand Docking) software (version 5.6.1), and docking coordinates were optimized around a single solvent-accessible site. A total of 100 confirmations were generated for each ligand in a sample of 330 compounds. The GOLD scoring function was utilised to rank each ligand pose. The following equation is used to get the gold score.

GOLD Fitness = Score (hb_ext) + Score (vdw_ext) + Score (hb_int) + Score (vdw_int)

Here, hb_ext and vdw_ext represent the protein-ligand H-bond and van der Waals interaction. Further, hb_int and vdw _int shows intramolecular hydrogen bonds in the ligand. A detail analysis of the docked confirmations was performed to obtain the final confirmation. Both the ligand and protein were considered flexible by performing a total of 100 genetic algorithm runs per molecule using the gold score fitness function to enhance the conformational space. The best pose was selected for each molecule to explore the protein ligand interactions inside the binding cavity of CACNA1G. These 330 poses of each ligand were then used for virtual screening in ligand scout for further analysis of our data.

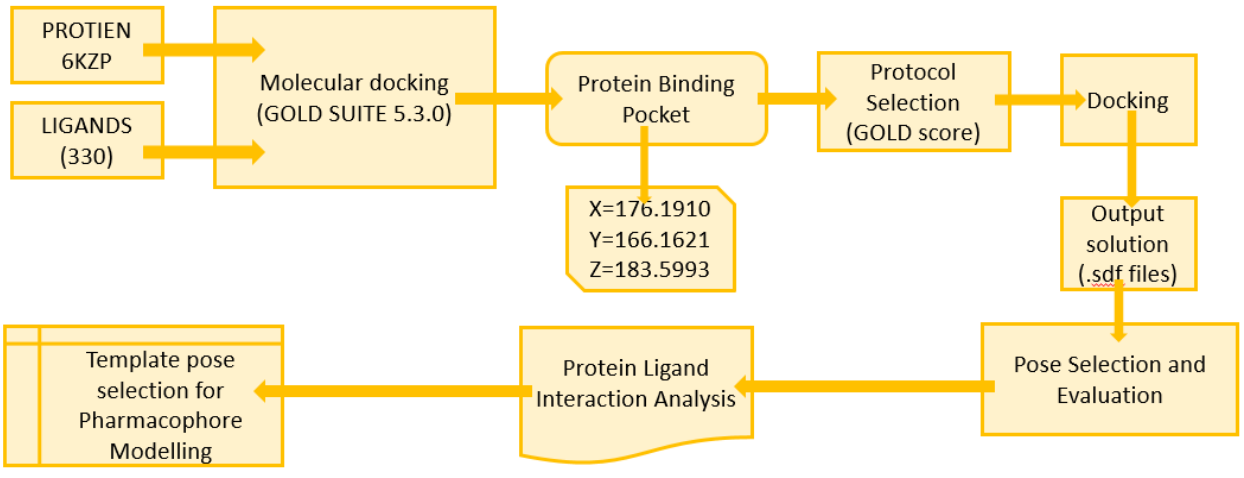

Figure 9: Overall work flow of Molecular docking

3.5 Machine Learning

3.5.1 Data Collection

A structurally diverse dataset of 524 ligands of calcium channel CNAC1G, along with their biological activity (IC_{50}) values were retrieved from literature and chemical databases (CHEMBL and PubChem)(48)/ Subsequently, duplicates, racemic compounds and fragments were discarded. Moreover, the compounds having molecular weight less than 200 were removed from the data as they reflect molecular fragment. After the exploration of the preliminary models, it was observed that the inhibitory potency (IC_{50}) values for the dataset were discrete and the numerical difference was quite large, that results in a poor model effect. Therefore, pIC_{50} values were calculated by taking negative logarithm of IC_{50} to the base 10. The SMILES codes and the activity values (pIC_{50}) of CACNA1G inhibitors were collected from CHEMBL database.

3.5.2 Descriptors Computation and feature Selection

Molecular descriptors are the end result of logical and mathematical process which converts chemical information encoded by symbolic representation into a useful output (numbers)[222]. In this study, MOE (Molecular Operating Environment) was used to compute a total of 206 descriptors for all EGFR modulators to identify the relationship between activity and molecular structure. Total of 205 descriptors were computed and three refinements criteria were applied for the attribute selection. These include the removal of variables with: (i) zero values (ii) Small variance <0.5 (for the removal of variables with same values) (iii) high correlation r >0.5(for the removal of variables containing same information). the dataset was divided into 80% training and 20% test set data in order to evaluate the predicted performance of the models on the basis of diverse subset selection method. Additionally, after the preprocessing, the dataset of 330 ligands was collected, the inhibitors dataset was divided into two activity levels including active, and inactive. Actives were divided having IC_{50} value less than 1000nM whereas in actives were compounds having activity value greater or equal to 1000nM.

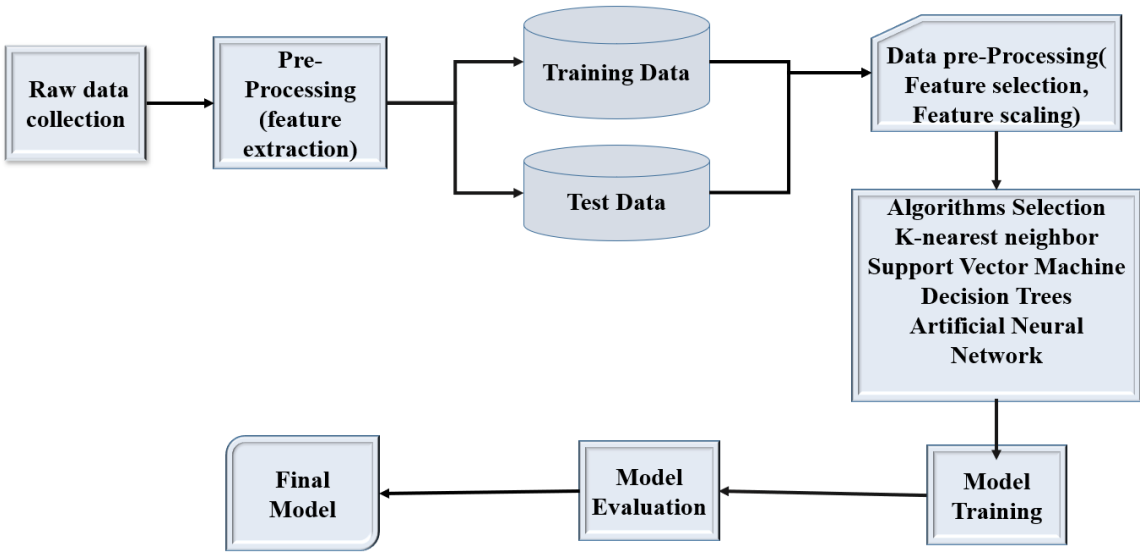

Figure 10: Overall workflow of Machine learning

3.5.3 Decision Tree

The decision tree model for the classification of active and inactive inhibitors of CACNA1G was built using the refined set of already calculated 2D descriptors. Herein, the classification procedure was optimized, and it was observed that the J48 classifier predicted a better model (high accuracy) as compared to other classifiers including Random Forest and Random Tree. Therefore, the J48 classifier in the WEKA software package (49) was finally used to develop decision tree. A J48 classifier is an improved version of C4.5 algorithms that creates a binary decision tree to model the classification procedure based on the divide-and-conquer rule.

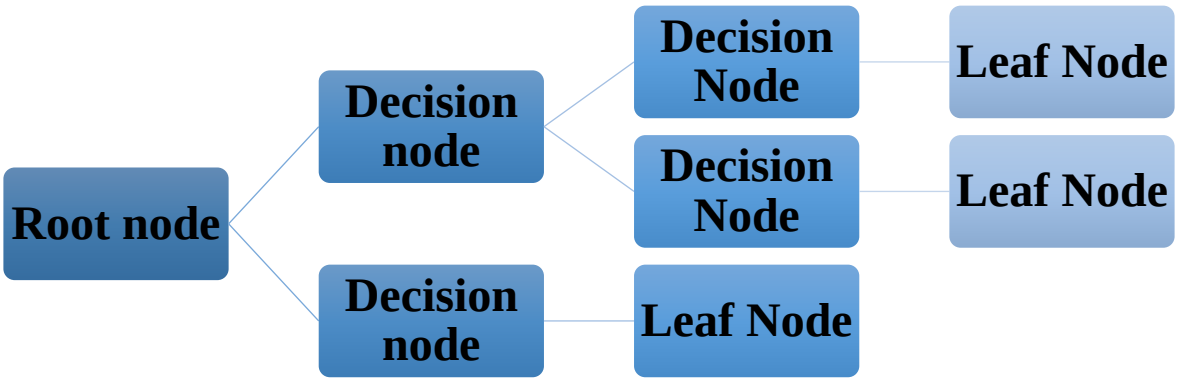

Figure 11: Overall workflow of Decision Tree

3.5.4 Artificial Neural Network (ANN)

In this study, a multi-layer perception (MLP approach was used to further classify the active and inactive inhibitors of CACNA1G. WEKA software package(49)] was used to construct the one-layer MLP based on the decision tree extracted . The neurons of input layer include all the independent variables (2D descriptors extracted from decision tree) and the neurons of the output layer include dependent variable (i.e. CACNA1G inhibitors activity label). Each neural network was initialized with random parameters and then trained by modulating the hidden layer, learning rate and momentum of the data set to optimize the model. In order to achieve the most optimized model, validation was performed using the test set Moreover, the choice of the number of hidden layers and learning rate is a vital decision to be considered when designing M`LP-ANNs. After the optimization, when a network achieves better performance in the internal validation data set, the parameter values were further selected for the test set validation

Here, test set was used to ensure that the built CANCNA1G model displays good generalization ability and better performance. It is extremely critical to quantitatively evaluate the effectiveness of the decision tree and artificial neural network models. Therefore, accuracy (Acc), specificity (TP) and sensitivity (TN) parameters represented in eq. 3, 4 and 5 were calculated for the predicted models to evaluate the overall performance of the models. Accuracy represents the number of correct predictions to the total number of predictions of CACNA1G inhibitors dataset. (Moreover, the specificity and sensitivity represent the number of correctly predicted CACNA1G inhibitors from the class of actives and inactive, respectively.

$$\text{Accuracy(Acc)} = \frac{(\text{TP}+\text{TN})}{\text{TP}+\text{TN}+\text{FP}+\text{FN}} \quad (3)$$

$$\text{Sensitivity (TP)} = \frac{\text{TP}}{\text{TP}+\text{FN}} \quad (4)$$

$$\text{Specificity (TN)} = \frac{\text{TN}}{\text{TN}+\text{FP}} \quad (5)$$

Matthews correlation coefficient (MMC) was used to further evaluate the model as it takes benefit of all the four variables (TP, TN, FP, FN) thus, providing a more balanced, representative and comprehensive measure as shown by eq. 6. The MCC value ranges

from -1 to 1, where 1 represents the perfect correlation between the actual and predicted response of the class.

$$MCC = \frac{(TP \times TN) - (FP \times FN)}{\sqrt{(TP+FP)(TP+FN)(TN+FP)(TN+FN)}} \quad (6)$$

3.6 Pharmacophore Modelling

A pharmacophore model is defined as "an ensemble of steric and electronic characteristics required to enable optimum supramolecular interactions with a given biological target and to initiate (or inhibit) its biological response." Pharmacophore model was made using ligand scout v4.

In ligand scout (50)ligand template which was the best docked pose with macromolecule was loaded and a pharmacophore was created. Based on features like Hydrophobic (Hyd), Donor and Acceptor (Don&Acc), Hydrogen bond Donors (Don>0.6), Aromatic rings (Aro), and Hydrogen bond Acceptors (Acc>0.8), the model discriminates the actives ligand from inactive. Therefore, with the help of a stable active ligand, the pharmacophore model was build. After generation of pharmacophore by ligand scout, pharmacophore was copied to alignment perspective for better view of results and then from alignment perspective it was copy to screening perspective.

In screening perspective database was first created in which docked 330 ligand poses were present and then it was loaded in ligand scout and was screened out. . By evaluating the number of actives and in actives in the internal hits, model validation of the respected pharmacophore model was made. This step was crucial to predict the reliability of a model. Therefore, a confusion matrix algorithm was used to classify the dataset. Those ligands which are actives (IC_{50}<1000nM) and predicted active by the pharmacophore model were stated as True Positives (TP). Similarly, True Negatives (TN) were those inactive ligands (IC_{50}>1000nM) that were predicted as inactive by model. While those ones that are actives in nature but do not appear in hits, i.e., predicted as inactives, were False Negatives (FN). Likewise, False Positives (FP) were those ligands that were inactive but recognized as actives by the model.

After classification of ligands, evaluations were made on certain statistical parameters such as Specificity (true negative rate), Sensitivity (true positive rate), Accuracy (overall prediction rate), and Precision (positively predicted values). However, the decision was clarified on the basis of Matthews Correlation Coefficient (MCC), which correlated the actual and predicted value by taking all classified variables (TP, TN, FP, and FN). The model was predicted best by its prediction statistics and utilized further for the virtual screening of different libraries.

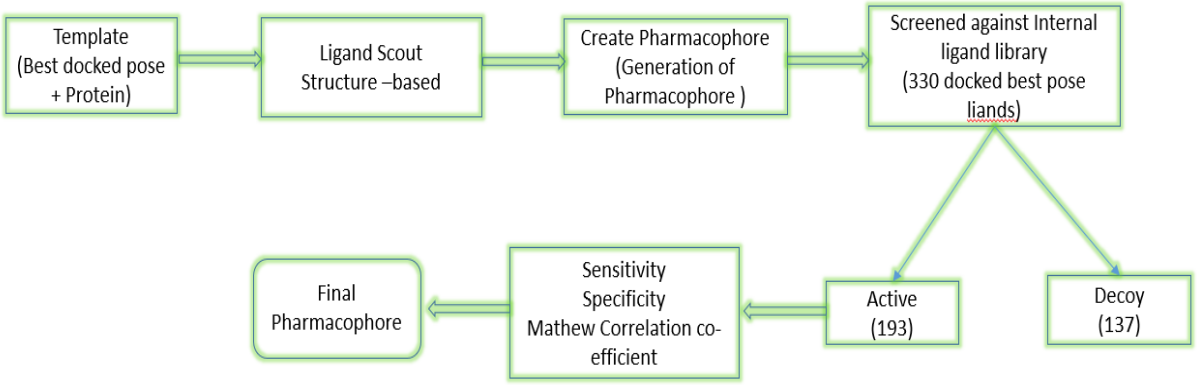

Figure 12: Overall workflow of pharmacophore Modelling

3.7. Virtual Screening

Virtual screening (VS) is a drug discovery approach that searches libraries of small molecules for structures that are most likely to bind to a therapeutic target, generally a protein receptor or enzyme. For this purpose the three databases were organized and The first library was prepared by taking data for all online FDA-approved medicine that has been used for neuroblastoma. The second library was extracted from Drug Bank Database [(51)], an online repository for all FDA approved drugs (10631). In contrast, the third one is retrieved from the commercially available natural compounds database, i.e., the ZINC Database [89]. These databases were then individually screened against CYP's model to evaluate the metabolic activities of the compounds. The filter is commercially available at the Online Chemical database server (ochem.eu), consists of a further 5 CYP's models such as CYP2C19, CYP2C9, CYP1A2, CYP2D6, and CYP3A4 to screen out the compound, effectively. The compounds screened from the model were stated as the non-inhibitors of CYP. The non-inhibitors obtained from the above screening then passed through in-house hERG pharmacophore model (add ref), a cardiotoxicity prediction model

prepared by Dr. Saba Munawar. The non-hits of the model were declared to be nontoxic against the hERG channel. The selected compounds then screened against best-featured model to identify the most potent external hits. Finally, the hits from the CACNA1G model proposed as effective and safer leads against CACNA1G.

CHAPTER 04

RESULTS

4.1 Data Collection

The PDB ID: 6KZP of our protein was downloaded from PDB bank. (10.2210/pdb6kzp/pdb)

Cleaning of co-crystallize structure of CACNA1G was done using MOE which include

removal of attached ligands along with atoms. Furthermore, active binding side was identified as shown in figure below along with binding residues.

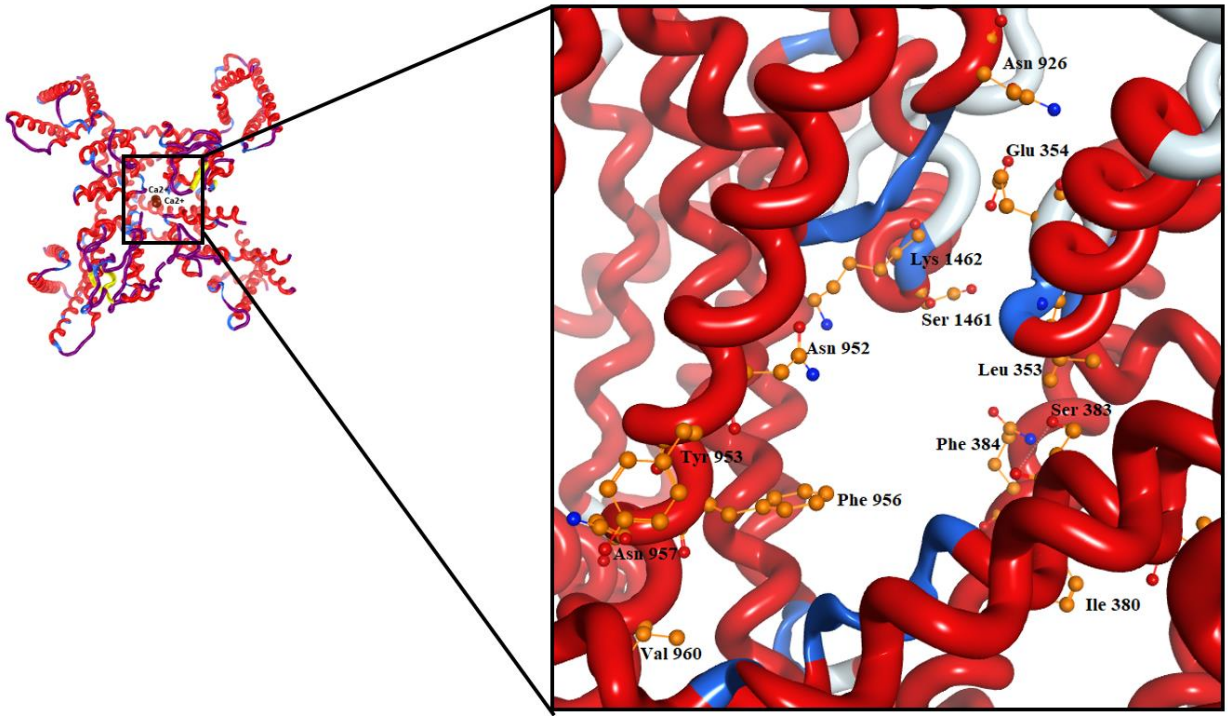

Figure 13 : X-ray crystallographic Structure of CACNA1G along with binding residues identified in binding pocket.

4.2 Molecular docking

The dataset of CACNA1G (330 compounds) were initially energy minimized by Amber 10 force field. Then these energies minimized compounds were used in molecular docking against CACNA1G to assess their inhibitory properties. For the site-specific docking it is crucial to include all the active and binding residues within the binding cavity of protein. Hence, around 10A^{o} region, X=176.1910, Y=166.1621 and Z=183.5993 coordinates for 1KZP has been selected for binding cavity. the active site was found at the II–III fenestration to be a specific drug-binding site. The fenestrations, owing to their relatively lower sequence conservation, thus represent specific druggable sites. Moreover, by keeping the ligand and side chains of protein flexible, molecular docking approximately provided 100 poses per compound as an output for CACNA1G. Later on, top pose was selected of each 330 ligand based on correlation between gold fitness score and pIC_{50} values. A database of top 330 docked ligand poses was created which was later to be used

in pharmacophore modelling. The picture below show all the 330 ligands docked in binding cavity of protein and to see common interaction PLIF analysis was done.

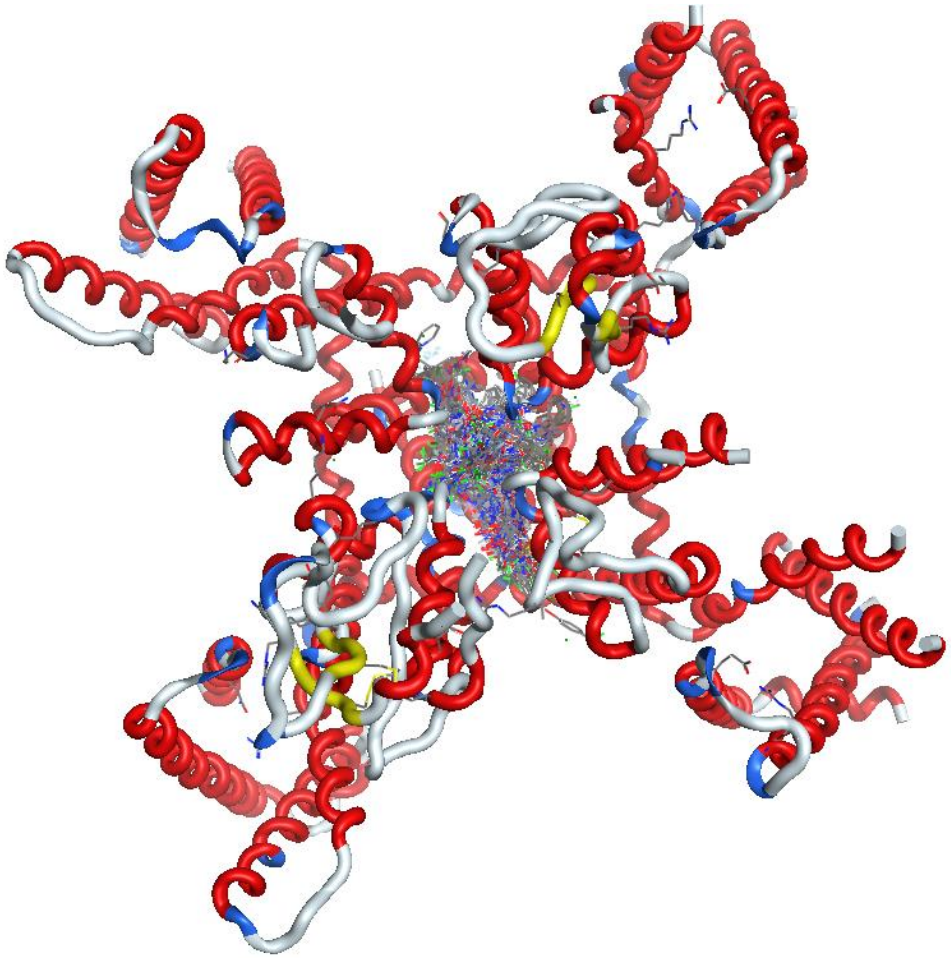

Figure 14: Docked 330 ligands in binding cavity area of CACNA1G (1KZP)

4.3 PLIF Analysis

For protein-ligand interaction analysis, one confirmation with best score for each ligand was selected and analyzed with the help of protein-ligand interaction fingerprint (PLIF). MOE software was used for calculation of PLIF for each ligand which explains about binding pattern of data in collective way along with type of interactions for single amino acid. PLIF explains the occurrence frequency of interaction type in each complex taking into account side chain Hydrogen Bond Acceptor (HBA), side chain Hydrogen Bond donor (HBD), backbone hydrogen bond donor (HBd), backbone hydrogen bond acceptor (HBa) and surface contacts (SAC). All ligands occupy the binding pocket in the 1KPZ. PLIF analysis indicates that Leu353 is the most commonly occurring interaction in 57.5% (188

ligands) of the data and Gln922 interaction has been showed that majority ligands show interaction with this residue. Likewise, Gln1816 and Phe 384 interaction are also important, and majority found in binding. Both Leu 353 and Gln922 interaction were also reported in literature as the important binding interaction of CACNA1G inhibitors. Other important interactions include Phe384, Gln1816 and Asn952. Common interactions have been depicted in the figure.

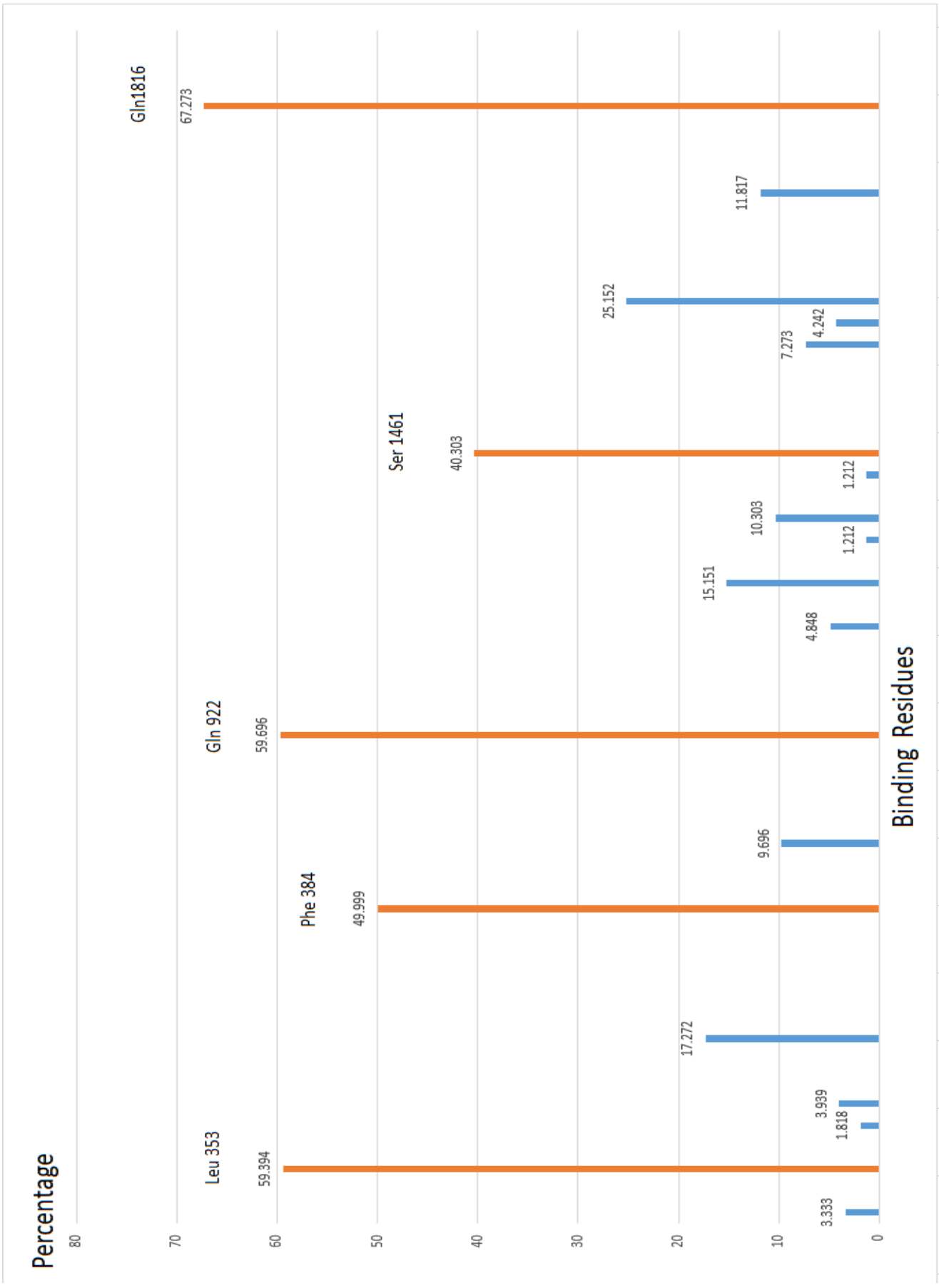
Percentage
80
70
60
50
40
30
20
10
0
Leu 353
59.394
3.333
1.818
3.939
17.272
Phe 384
49.999
9.696
Gln 922
59.696
4.848
15.151
1.212
10.303
Ser 1461
40.303
1.212
25.152
7.273
4.242
Gln1816
67.273
11.817
Binding Residues

Figure 15: PLIF analysis showing maximum interaction done with binding site residues

4.4 Machine Learning

4.4.1 Data Collection and Curation

Data set of filtered 330 ligands was used along with all the 206 descriptors computed while using MOE. The data set was divided into Training set (80 percent) which consists of 264 ligands whereas test set (20 percent) consisted of 66 ligands. Furthermore, an activity threshold was established such that the compounds having $IC_{50} \leq 1000$ nM considered as actives while compounds having $IC_{50} > 1000$ nM as inactive or least actives. pIC_{50} values of the whole data set was calculated according to the biological criterion to make the interpretation easier. Training set contains 154 actives and labelled as "1" while there were 110 inactive compounds labelled as "0" to be used as binary input in machine learning techniques.

Table 4: Table showing division of data containing actives and inactives

	Number of Compounds	Actives	Inactives
Training data set	264	154	110
Test Data set	66	40	26

4.4.2 Decision Tree

Decision tree classification model was constructed using built in J-48 decision making classifier algorithm of WEKA. All the 264 ligands along with 206 descriptors was given as the input after removal of descriptors having (i) zero values (ii) Small variance <0.5 (for the removal of variables with same values) (iii) high correlation r >0.5(for the removal of variables containing same information. Model showed significant statistical parameters along with excellent predictive (96.59%) ability as shown in table 4.4. Our model could classify 225 compounds correctly only 9 compounds (3.4 %) were not predicted correctly. Training set contained 154 active (1) ligands along with 110 inactive (0) ligands and the trained decision tree was efficient enough to predict 149 active ligands and 106 inactive correctly. The confusion matrix obtained from training set is given in table 6**.**

Our tree selected 16 essential descriptors necessary for building our model whose details are listed in table below.

Table 05: Descriptors selected by Decision tree along with the description

2D Descriptors	Description
SMR_VSA6	Sum of van der Waals surface area where the contribution to SMR is in the range (0.485,0.56)
Vsa_other	MOE descriptor that consider only heavy atoms of a molecule and Approximation to the sum of VDW surface areas ($Å^2$) of atoms typed as "other".
PEOP_VSA-6	Sum of van der Waals surface area where partial charge is less than –0.30.
PEOP_VSA-1	Sum of van der Waals surface area where partial charge is in the range (–0.10,– 0.05)
b-double	Number of double bonds. Aromatic bonds are not considered to be double bonds.
Chiral-u	The number of unconstrained chiral centers.
Opr_nrot	The number of rotatable bonds
a_Nf	Number of fluorine atoms: $\#\{Z_i \mid Z_i = 9\}$.
PEOE-VSA-2	MOE descriptor of Partial Equalization of Orbital Electronegativities (PEOE) where Sum of wander waal area v_i where and partial charge of atom q_i is greater than 0.3.
h_pstrain	The strain energy (kcal/mol) needed to convert all protonation states into the input protonation state
a_aro	Number of aromatic atoms.
b_max1len	Length of the longest single bond chain
SMR_vsa_4	Sum of van der Waals surface area where the contribution to SMR is in the range (0.1,0.15)
lip _violation	The number of violations of Lipinski's Rule of Five
Radius	Smallest entry in the distance matrix
PEOP-vsa_6	Sum of van der Waals surface area where partial charge is greater than 0.30
PEOP_vsa_PNEG	Total negative polar van der Waals surface area
Chi1V_c	Carbon valence connectivity index (order 1)

Table 06: Result of decision tree model on Training data

	TP RATE	FP RATE	PRECISION	MCC
Inactive	0.964	0.032	0.955	0.9330

Actives	0.968	0.036	0.966	0.930

Table 07: Confusion Matrix of Training data

N=264	**Predicted Inactive(0)**	**Predicted Active(1)**	
Actual Inactive (0)	106	4	110
Actual Actives(1)	5	149	154
Total	111	153	**264**

The above table showed very good statistical results of our training data. To validate the model of decision tree test set was used which consisted of 40 actives and 26 inactive compounds. Our model was able to predict 63 compounds (95.45%) correctly whereas only 3 compounds (4.5%) were incorrectly classified. The table below show the results of our model being validated through test set .

Table 08: Result of decision tree model on Test data

	TP RATE	**FP RATE**	**PRECISION**	**MCC**
Inactive	0.962	0.050	0.926	0.906
Actives	0.950	0.038	0.955	0.906

Table 09: Confusion Matrix of Test data

N=66	**Predicted Inactive(0)**	**Predicted Active(1)**	
Actual Inactive (0)	25	1	26
Actual Actives(1)	2	38	40
Total	27	39	**66**

When we compare the results of both test and training sets model we can see that our model accuracy is high and giving best results about 96 percent of accuracy which shows our model is able to classify active and inactive ligands.

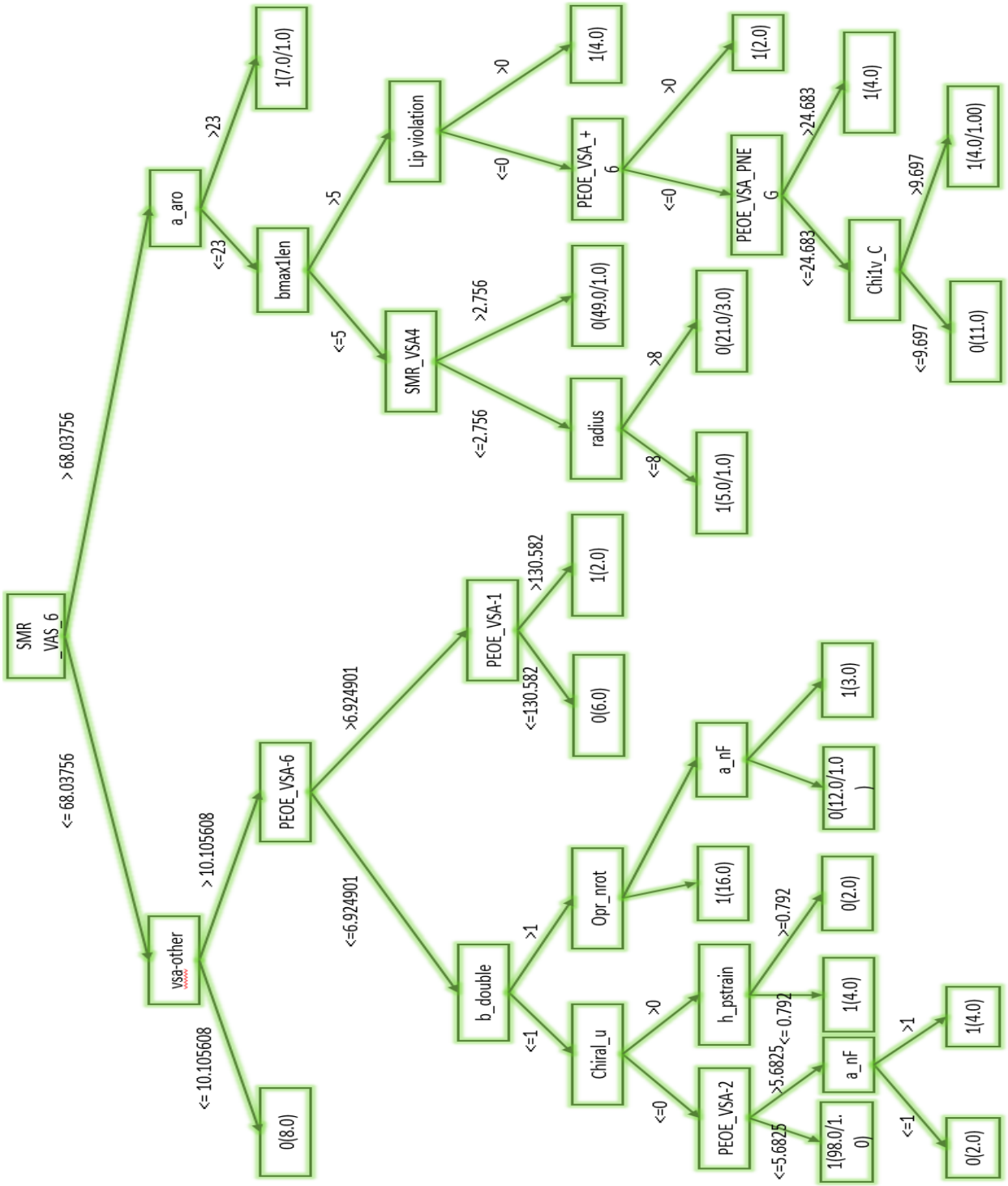

Figure 16: Decision tree classification model

4.4.3 SVM

In order to test our model results we made another classification model where above mentioned 16 descriptors selected by Decision tree were used as an input to make our

classification model for accuracy. Different models were generated using different descriptors via multilayer perception classifier on WEKA. A neural network model with 96.2% accuracy and a good predictive ability was achieved by using 17 2D descriptors. The final neural network contains 17 input nodes, 9 hidden nodes and two output; labelled as 1 for active class of compounds and 0 for inactive class. The leaning rate for training model set at 0.3 and momentum at 0.2. The model was efficient enough to correctly classify 96.2 % of the data and only few compounds were misclassified by this predictive model as shown in table 4.6.

Of all compounds 254 were classified correctly however only 10 ligands were not classified correctly. As sensitivity measure the true positive rate was observed to be 96.2% which means only 3 out of 154 active compounds were not predicted correctly making FP = 3. Moreover, the specificity (true negative rate) was 93% which implies that out of total 110 inactive compounds only 7 were misclassified making FN = 5. Confusion matrix generated for training set is tabulated in table 10.

Table 10: Results of SVM training data set

	TP RATE	**FP RATE**	**PRECISION**	**MCC**
Inactive	0.936	0.019	0.972	0.922
Actives	0.981	0.064	0.956	0.922

Table 11: Confusion Matrix of SVM training data set

N=264	**Predicted Inactive(0)**	**Predicted Active(1)**	
Actual Inactive (0)	103	7	110
Actual Actives(1)	3	151	154
Total	106	158	**264**

In order to validate our training model test, set of 66 ligands containing 40 actives and 26 inactive was used. Our model was able to classify with 100 percent accuracy. All 40 actives ligands were classified as actives whereas all inactive ligands were classified as inactive showing that our model is able to validate the training data statistics as well as is best model for classification. Below tables show the statistics and confusion matrix of test set used in Multilayer percepton.

Table 12: Results of SVM test data set

	TP RATE	FP RATE	PRECISION	MCC
Inactive	1	0	1	1
Actives	1	0	1	1

Table 13: Confusion Matrix of SVM test data set

N=264	Predicted Inactive(0)	Predicted Active(1)	Total
Actual Inactive (0)	26	0	20
Actual Actives(1)	0	46	46
Total	26	46	**66**

4.5 Pharmacophore Modelling

For pharmacophore Modelling in ligand scout, template was loaded in ligand scout which was best top docked pose from 330 molecules having PIC50 value=9.0nm.

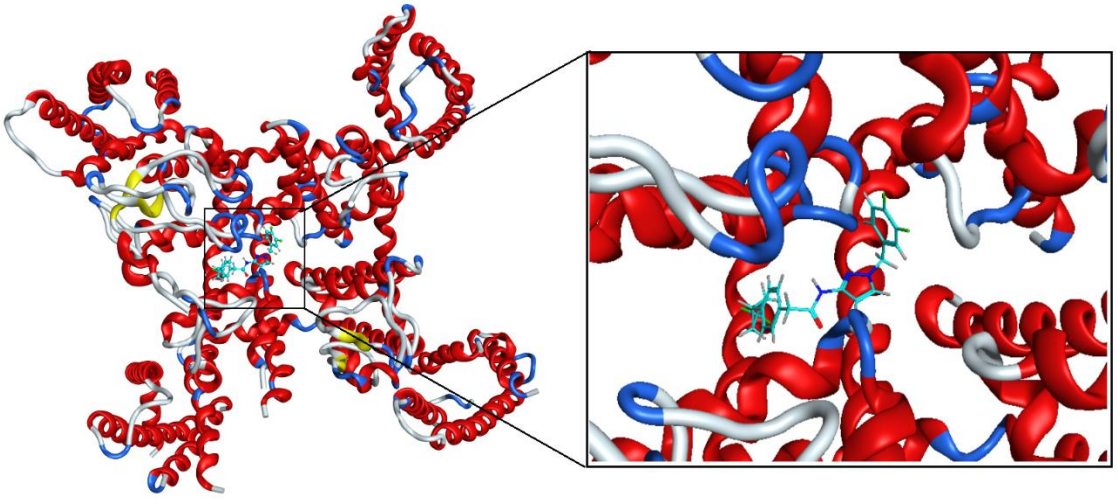

Figure 17: Structure of best docked pose of ligand in protein

The following picture show our ligand and protein in software in structure based modelling.

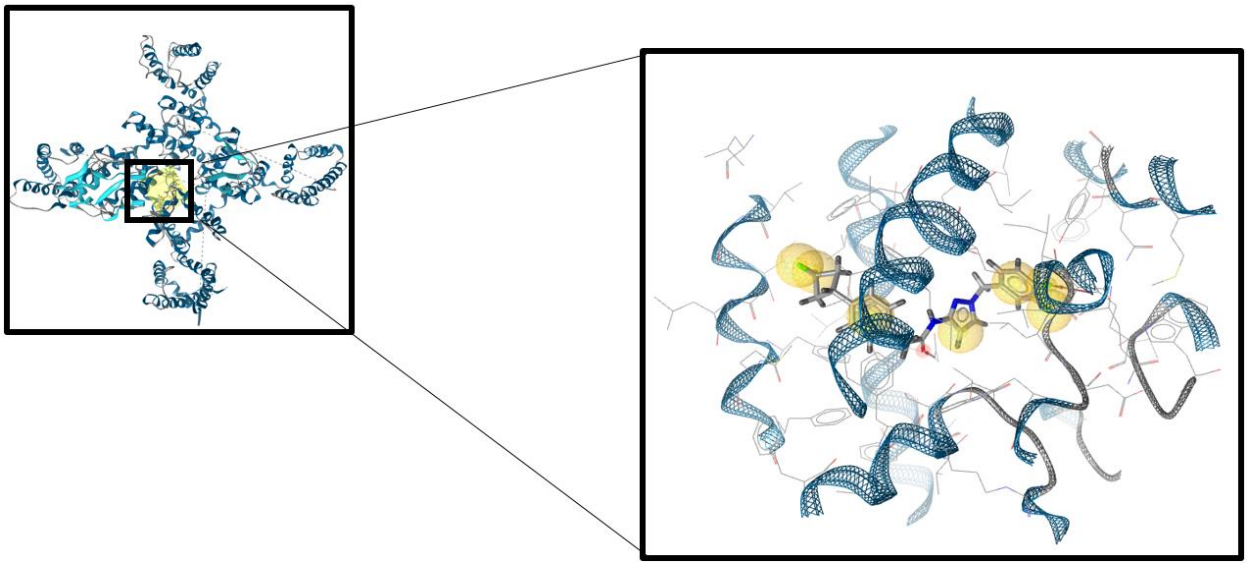

Figure 18: Structure of docked best pose of ligand in our protein 1KZP having pIC_{50} value=9.0nM. Dark blue color shows helices, Light blue color show strand whereas yellow cube shows our docked ligand in the binding cavity along with the highlighted pharmacophore

The below figure shows our template ligand selected along with binding residues and pharmacophore being created by ligand scout.

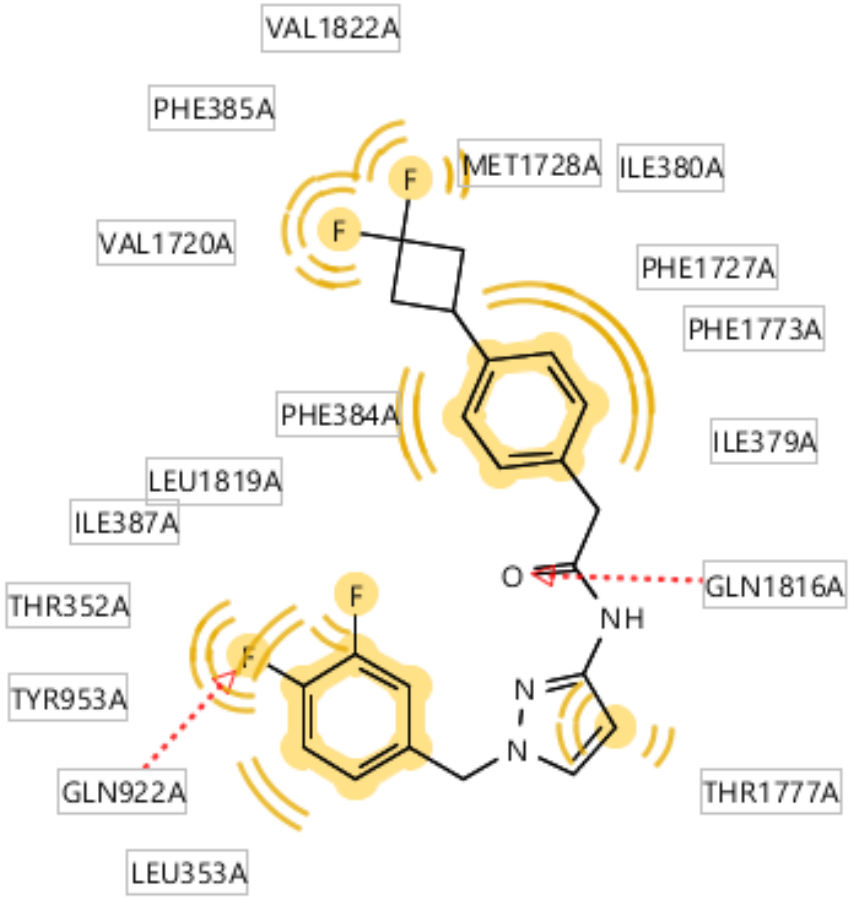

Figure 19: Figure of details of template ligand selected for pharmacophore modelling with bonding site residues. Yellow color shows Hydrophobic interaction and features with the residues whereas red arrow shows hydrogen bond acceptor feature.

Our pharmacophore model consisted of 9 pharmacophore features out which 2 were hydrogen bond acceptor and 7 were hydrophobic interactions.

Pharmacophore model validation

To validate our pharmacophore model, the pharmacophore model was then screened from the rest of the docked dataset for internal test validation. Before screening the number of minimum matching features with pharmacophore was set to 4 for classification of active ligands The model was able to classify the ligands as TP = 193, TN = 135, FP = 0 and FN =2. The statistics of the classification were then evaluated via a confusion matrix. The resultant of the matrix showed an accuracy of 99%, asserting that the pharmacophore

model was able to predict and classify the ligands as precisely (actives as actives, inactive as inactive). However, the value of precision and specificity or True Negative Rate (TNR), i.e., 1.000, declared that the model is specific. Similarly, the model's sensitivity or True Positive Rate (TPR) (0.98) indicated that the model is sensitive for all features associated with actives compounds (TP). The specificity of 1.000 declared that given feature predicted inactive more precisely as compared to actives (table 4.1).

Table 14: Statistical Evaluation of the Pharmacophore

Statistical approach	Implementation of results	Model Evaluation
Accuracy	= 195+135/195+135+0+2	0.99 = 99%
Sensitivity	= 195/195+2	0.9800
Specificity	= 135/135+0	1.000
Precision rate	= 195/195+0	1.000

Another statistical metric was employed to assess the model's predictive accuracy. The Matthews Correlation Coefficient (MCC) assesses the degree of agreement between anticipated and observed values. It is a correlation coefficient that takes all variables (TP, TN, FP, and FN) and offers model classification scores. A number close to or around 1 shows the best agreement between expected and actual responses. The MCC score for the pharmacophore model was 0.987, indicating that the selected template and all true positive drugs with related properties can suppress T-type calcium overexpression.

4.6 Virtual Screening

The evaluated model was then screened against the two external datasets. For this step, datasets from publicly accessible databases were retrieved and preprocessed. The first and second datasets consisted of chemical data from the Drug Bank Database (10631), ZINC Database (885). To evaluate the metabolic profiles of all chemical entities, the substrate from all databases were passed through CYP Model. The selected entries from the CYPs, i.e., 201 from Drug Bank Database, 303 from the ZINC database and 9 from EPI/SMA Database were identified as non-inhibitors of the CYPs. These compounds were then

screened against the in-house hERG pharmacophore model, to avoid cardiotoxicity. At the end of the query, 185 (Drug Bank database), 177 (ZINC database) were identified as non-inhibitors of hERG.

After ADMET toxicity analysis, the selected compounds were screened against the best-featured pharmacophore model. The resultant hits demonstrated that 8 compounds from the above listed database entries have potential features. These identified compounds could be effective and safer against neuroblastoma and therefore can be utilized further for lead optimization protocol.

Following below show our 6 hits which can be further used for drug repurposing

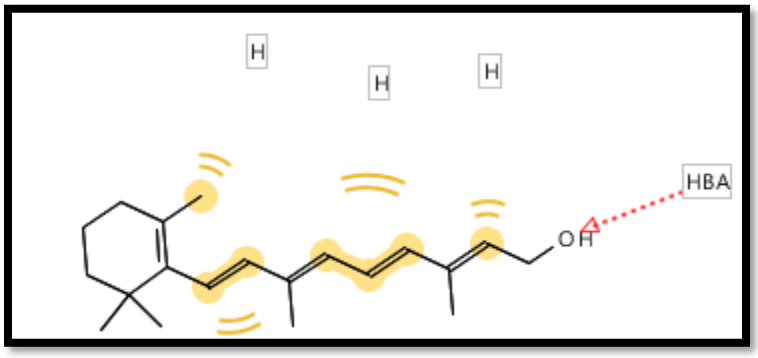

Vitamin A is a vitamin important for retinal function that is used clinically to correct vitamin A deficiency. In previous studies Treatment of both MYCN gene-amplified and non-amplified human neuroblastoma cell lines with all-trans-retinoic acid (ATRA) caused a marked decrease in MYCN RNA expression and arrest of cell proliferation. Vitamin A is used in neuroblastoma treatment and our identified target can also be used in treatment of Neuroblastoma.(52)

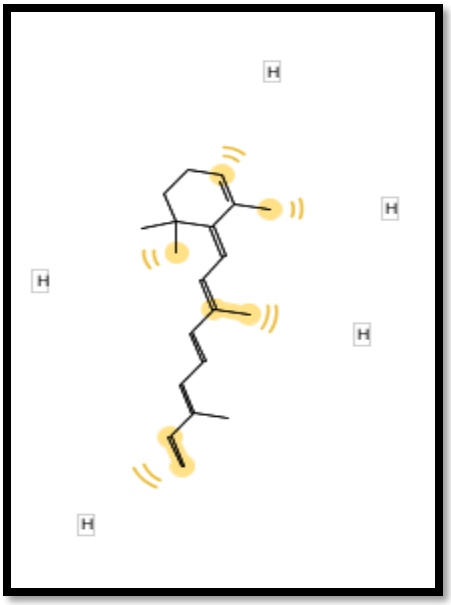

Beta carotene is a vitamin A precursor found in various nutritional supplements and health products and is an approved Drug. In clinical trials Cyclophosphamide this molecule is used is a nitrogen mustard used to treat lymphomas, myelomas, leukemia, mycosis fungoides, neuroblastoma, ovarian adenocarcinoma, retinoblastoma, and breast carcinoma. This identified drug can also be repurposed for treatment of neuroblastoma. (53)

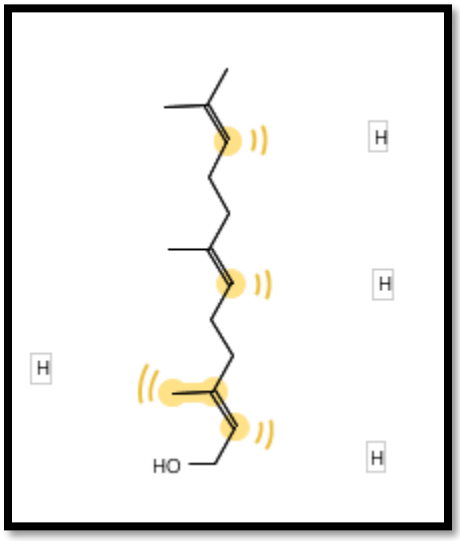

geraniol has also been shown to sensitize tumor cells to commonly used chemotherapies including Fluorouracil and Docetaxel and represents a promising cancer chemo preventive agent and can help to treat neuroblastoma as well. Amine oxidase [flavin-containing] B is

the target which activity is that it catalyzes the oxidative deamination of biogenic and xenobiotic amines and has important functions in the metabolism of neuroactive and vasoactive amines in the central nervous system and peripheral nervous system and our target is also related to abnormality in ion exchange i.e. calcium ion exchange due to calcium channel in nervous system so they might be related to each other and might be purposed as a drug or agent in neuroblastoma treatment. (39)

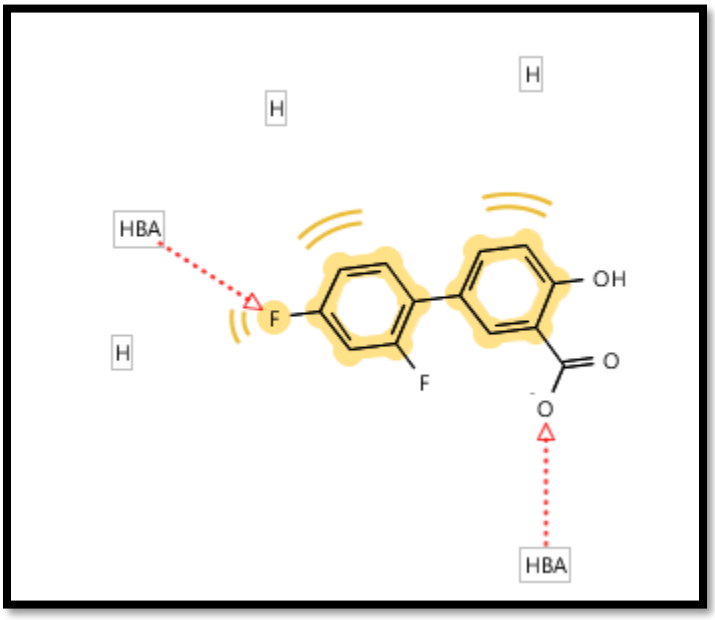

Diflunisal, a salicylate derivative, is a nonsteroidal anti-inflammatory agent (NSAIA) with pharmacologic actions similar to other prototypical NSAIAs. Diflunisal possesses anti-inflammatory, analgesic and antipyretic activity.

Prostaglandin G/H synthase 1 is its target which is involve in regulation of cell proliferation. Increased cell adhesion, phenotypic alterations, apoptosis resistance, and tumor angiogenesis are all linked to PTGS2 upregulation. In cancer cells, PTGS2 is a necessary step in the formation of prostaglandin E2 (PGE2), which regulates motility, growth, and apoptosis resistance.(54)

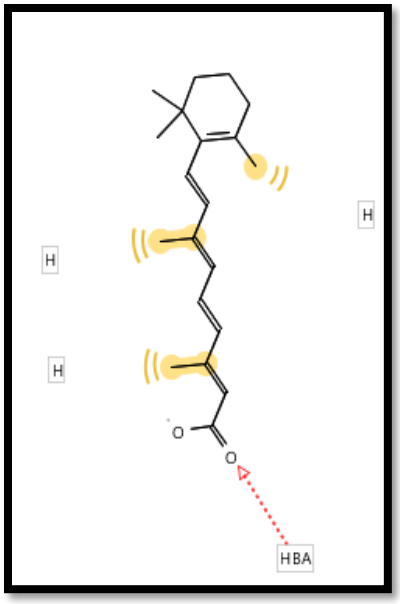

Alitretinoin is a key regulator of gene expression in neoplasms and throughout growth and development. Tretinoin, also known as retinoic acid, is a nutrient generated from maternal vitamin A that is required for optimal growth and development. Tretinoin in excess can cause teratogenic effects. It's used to treat psoriasis, acne vulgaris, and a variety of other skin conditions. It's also been authorized for the treatment of promyelocytic leukemia (acute promyelocytic leukemia).

There are 6 targets of Alitretinoin which help in gene expression and are related to our target in a way that due to over expression of CACNA1G gene there is more influx of calcium leading to cell proliferation a cancer. By using this drug for treatment of neuroblastoma there is a possibility that our gene gets down regulated and hence calcium influx is maintained. Moreover, retinoid treatment is used in treatment of neuroblastoma so these drugs can be repurposed for the therapy of neuroblastoma.

CHAPTER 5

DISCUSSION

Neuroblastoma is a disease which is caused by over expression of T type calcium channels which is basically a gene CACNA1G. This gene over expression is because of gene duplication in certain DNAs leading to neuroblastoma. Over expression of this gene leads to more influx of calcium ion in cell and lead to disruption of hemostasis of calcium signaling. In order to overcome this calcium ion blocker are design so that influx of calcium can be controlled. The first module performed was molecular docking module was performed in which our ligands data set was docked within the binding site of our protein PDB ID: 1KZP which showed that these ligands can be potential inhibitors of calcium channel but weak co relation between IC_{50} and docking score showed that our ligand interactions are not stable. To validate our stability of interactions PLIF analysis was done in which all the mentioned residues in section 3 were involve in binding with ligands. to validate our model data of actives and inactive ligands several classification models were built based on machine learning. 80% of our data was classified as training data rest 20 percent was used as a test set for validation of our model. The results of both test and training data in decision tree J-48 classifier showed good results around 95 percent of accuracy which showed our model was very good. Next Multilayer perceptron model was built in weak in which the filtered data set was used and only 17 descriptors were given as an input to avoid misclassification and low accuracy. The results of SVM on training and test data set also validated our model with 97 percent accuracy hence leading to validation of our decision tree model as well.

Pharmacophore modelling was done in order to identify the essential feature of our ligands hat are responsible for the biological activity. Using ligand scout Our pharmacophore was generated containing 2 hydrophobic aromatic, 4 hydrophobic aliphatic and 2 Hydrogen bond acceptors. This pharmacophore was further used for virtual screening against neuroblastomic drugs, FDA-approved drugs from different databases. Considering the pharmacokinetic properties, the compounds of these databases were assessed based on ADMET property. The compounds from the filters like CYPs and hERG (anti-target candidates) were expected to be non-carcinogen and non-toxic, thus reliable as potential inhibitors against the targeted protein and are proposed as potential leads for further in silico processing. From the previous studies Vitamin, A and retinoic acid isomers were

identified to treat high risk neuroblastomas. As they are known to inhibit the voltage gated calcium channels. It means we can use vitamin A precursors and retinoic acid to inhibit the voltage gated calcium channel activity. In one more study it was found that RA delayed rate of channel activation but increased rate of deactivation. This might be useful in neuroblastoma treatment as the overexpression of calcium channel may be suppressed by using RA and then it may lead to apoptosis instead of cell proliferation. When we see our residues involve in binding as well as shown in our pharmacophore that are GLU923A, ASP 1776 they are important binding residues for inhibition of calcium channel as they were also identified in previous studies to be important for binding of ligands in calcium channel.

CHAPTER 06

CONCLUSION

In the end we conclude that present study was focused on finding the potential inhibitors of calcium channel so that over influx of calcium ion can be controlled to avoid neuroblastoma. After molecular docking of 330 Ligands using GOLD suite we found out that residues Leu 353, Gln 922, Phe 384 and Gln 1816 were important residues identified to block the activity of CACNA1G which was found after PLIF analysis. Furthermore, template selection for pharmacophore modelling as done in which template with highest pIC50 =9.0Nm was selected. Using Ligand scout software our Pharmacophore model was built which identified all the important pharmacophore features responsible for enhancing the activity of ligands in blocking the activity of CACNA1 which included total features. 2 were Hydrogen bond acceptors and 7 were Hydrophobic interactions. Furthermore, our pharmacophore model of blocker of CACNA1G was screened against internal library which showed 99% accuracy in classifying the actives an in actives ligands data set. This model was further screened against Drug bank FDA Approved drugs and ZINC library of natural compounds out of which were filtered against CYP450 and resulting 201 non hits from Drug bank and 303 non-hits from ZNC were further screened out by our in hERG Model. The resultant left ligands were 185 non hits from Drug bank and 177 Non hits from Zinc Library which were further virtually screened against our pharmacophore model, and we got 8 hits out of which 3 are in experimental stages while rest 5 are been approved and deposited in Drug Bank. The hits which are either vitamin A or precursor of Vitamin A Like Beta Carotene and Alitretinoin validates the authenticity of our model and strengthens it as Vitamin A and its precursors are used in treatment of neuroblastoma. Geraniol and Diflunisal can be repurposed as eh drug for treatment of neuroblastoma as Geraniol is used in treatment of cancers and used to sensitize tumor cells. In case of Diflunisal which is used to treat arthritis and osteoporosis can be used for treatment of neuroblastoma because of its target known as Prostaglandin G/H synthase 1. In cancer cells, PTGS2 is a key step in the production of prostaglandin E2 (PGE2), which plays important roles in modulating motility, proliferation and resistance to apoptosis. So, by targeting it we can induce apoptosis in neuroblastoma as well.

The machine learning module done in study helps us to conclude that our ANN model built by selective features of decision tree J-48 outperforms and classify CACNA1G inhibitors with accuracy above 90% on training set and 100 % accuracy on test set.

CHAPTER 07

REFERENCES

1. Brodeur GM. Neuroblastoma: biological insights into a clinical enigma. Nature reviews cancer. 2003;3(3):203–16.

2. Louis CU, Shohet JM. Neuroblastoma: molecular pathogenesis and therapy. Annual review of medicine. 2015;66:49–63.

3. Janoueix-Lerosey I, Schleiermacher G, Delattre O. Molecular pathogenesis of peripheral neuroblastic tumors. Oncogene. 2010;29(11):1566–79.

4. Kramer S, Ward E, Meadows AT, Malone KE. Medical and drug risk factors associated with neuroblastoma: a case-control study. Journal of the National Cancer Institute. 1987;78(5):797–804.

5. L Megison M, A Gillory L, A Beierle E. Cell survival signaling in neuroblastoma. Anti-Cancer Agents in Medicinal Chemistry (Formerly Current Medicinal Chemistry-Anti-Cancer Agents). 2013;13(4):563–75.

6. Colon NC, Chung DH. Neuroblastoma. Advances in pediatrics. 2011;58(1):297–311.

7. Orbach D, Sarnacki S, Brisse HJ, Gauthier-Villars M, Jarreau P-H, Tsatsaris V, et al. Neonatal cancer. The Lancet Oncology. 2013;14(13):e609–20.

8. Maris JM, Matthay KK. Molecular biology of neuroblastoma. Journal of clinical oncology. 1999;17(7):2264.

9. Park JR, Eggert A, Caron H. Neuroblastoma: biology, prognosis, and treatment. Pediatric Clinics of North America. 2008;55(1):97–120.

10. Schwab M, Westermann F, Hero B, Berthold F. Neuroblastoma: biology and molecular and chromosomal pathology. The lancet oncology. 2003;4(8):472–80.

11. Shohet JM, Nuchtern JG. Epidemiology, pathogenesis, and pathology of neuroblastoma. Hentet fra. 2016;

12. Brodeur GM, Nakagawara A. Molecular basis of clinical heterogeneity in neuroblastoma. The American journal of pediatric hematology/oncology. 1992;14(2):111–6.

13. Ribelles AJ, Barberá S, Yáñez Y, Gargallo P, Segura V, Juan B, et al. Clinical features of neuroblastoma with 11q deletion: an increase in relapse probabilities in localized and 4S stages. Scientific reports. 2019;9(1):1–9.

14. Shimada H, Ambros IM, Dehner LP, Hata J, Joshi V V, Roald B. Terminology and morphologic criteria of neuroblastic tumors: recommendations by the International Neuroblastoma Pathology Committee. Cancer: Interdisciplinary International Journal of the American Cancer Society. 1999;86(2):349–63.

15. Peuchmaur M, d'Amore ESG, Joshi V V, Hata J, Roald B, Dehner LP, et al. Revision of the International Neuroblastoma Pathology Classification: confirmation of favorable and unfavorable prognostic subsets in ganglioneuroblastoma, nodular. Cancer: Interdisciplinary International Journal of the American Cancer Society. 2003;98(10):2274–81.

16. Ho R, Minturn JE, Hishiki T, Zhao H, Wang Q, Cnaan A, et al. Proliferation of human neuroblastomas mediated by the epidermal growth factor receptor. Cancer research. 2005;65(21):9868–75.

17. Johnsen JI, Segerström L, Orrego A, Elfman L, Henriksson M, Kågedal B, et al. Inhibitors of mammalian target of rapamycin downregulate MYCN protein expression and inhibit neuroblastoma growth in vitro and in vivo. Oncogene. 2008;27(20):2910–22.

18. Brodeur GM, Seeger RC, Schwab M, Varmus HE, Bishop JM. Amplification of N-myc in untreated human neuroblastomas correlates with advanced disease stage. Science. 1984;224(4653):1121–4.

19. Johnsen JI, Dyberg C, Fransson S, Wickström M. Molecular mechanisms and therapeutic targets in neuroblastoma. Pharmacological research. 2018;131:164–76.

20. Ohkubo T, Yamazaki J. T-type voltage-activated calcium channel Cav3. 1, but not Cav3. 2, is involved in the inhibition of proliferation and apoptosis in MCF-7 human breast cancer cells. International journal of oncology. 2012;41(1):267–75.

21. Van Roy N, De Preter K, Hoebeeck J, Van Maerken T, Pattyn F, Mestdagh P, et al. The emerging molecular pathogenesis of neuroblastoma: implications for improved risk assessment and targeted therapy. Genome medicine. 2009;1(7):1–11.

22. Latour I, Louw DF, Beedle AM, Hamid J, Sutherland GR, Zamponi GW. Expression of T-type calcium channel splice variants in human glioma. Glia. 2004;48(2):112–9.

23. Bertolesi GE, Jollimore CAB, Shi C, Elbaum L, Denovan-Wright EM, Barnes S, et al. Regulation of α1G T-type calcium channel gene (CACNA1G) expression during neuronal differentiation. European Journal of Neuroscience. 2003;17(9):1802–10.

24. Lavie Y, Cao H, Bursten SL, Giuliano AE, Cabot MC. Accumulation of glucosylceramides in multidrug-resistant cancer cells. Journal of Biological Chemistry. 1996;271(32):19530–6.

25. Panner A, Wurster RD. T-type calcium channels and tumor proliferation. Cell calcium. 2006;40(2):253–9.

26. Morris SW, Kirstein MN, Valentine MB, Dittmer KG, Shapiro DN, Saltman DL, et al. Fusion of a kinase gene, ALK, to a nucleolar protein gene, NPM, in non-Hodgkin's lymphoma. Science. 1994;263(5151):1281–4.

27. Gackiere F, Bidaux G, Delcourt P, Van Coppenolle F, Katsogiannou M, Dewailly E, et al. CaV3. 2 T-type calcium channels are involved in calcium-dependent secretion of neuroendocrine prostate cancer cells. Journal of Biological Chemistry. 2008;283(15):10162–73.

28. Weaver EM, Zamora FJ, Puplampu-Dove YA, Kiessu E, Hearne JL, Martin-Caraballo M. Regulation of T-type calcium channel expression by sodium butyrate in prostate cancer cells. European journal of pharmacology. 2015;749:20–31.

29. McRory JE, Santi CM, Hamming KSC, Mezeyova J, Sutton KG, Baillie DL, et al. Molecular and functional characterization of a family of rat brain T-type calcium channels. Journal of Biological Chemistry. 2001;276(6):3999–4011.

30. Perez-Reyes E, Cribbs LL, Daud A, Lacerda AE, Barclay J, Williamson MP, et al. Molecular characterization of a neuronal low-voltage-activated T-type calcium channel. Nature. 1998;391(6670):896–900.

31. Hertwig F, Peifer M, Fischer M. Telomere maintenance is pivotal for high-risk neuroblastoma. Cell Cycle. 2016;15(3):311–2.

32. Fink CC, Slepchenko B, Moraru II, Watras J, Schaff JC, Loew LM. An image-based model of calcium waves in differentiated neuroblastoma cells. Biophysical Journal. 2000;79(1):163–83.

33. Berridge MJ, Whitaker M, Patel R, Kahl CR, Means AR, Humeau J, et al. Regulation of cell cycle progression by calcium/calmodulin-dependent pathways. Bioessays. 1995;70(6):3–15.

34. Lange I, Koster J, Koomoa D-LT. Calcium signaling regulates fundamental processes involved in Neuroblastoma progression. Cell calcium. 2019;82:102052.

35. Kifor O, Diaz R, Butters R, Brown EM. The Ca2+-sensing receptor (CaR) activates phospholipases C, A2, and D in bovine parathyroid and CaR-transfected, human embryonic kidney (HEK293) cells. Journal of Bone and Mineral Research. 1997;12(5):715–25.

36. Parkash J, Chaudhry MA, Rhoten WB. Calbindin-D28k and calcium sensing receptor cooperate in MCF-7 human breast cancer cells. International journal of oncology. 2004;24(5):1111–9.

37. Maris JM, Weiss MJ, Mosse Y, Hii G, Guo C, White PS, et al. Evidence for a hereditary neuroblastoma predisposition locus at chromosome 16p12–13. Cancer research. 2002;62(22):6651–8.

38. Günes DA, Florea A-M, Splettstoesser F, Büsselberg D. Co-application of arsenic trioxide (As2O3) and cisplatin (CDDP) on human SY-5Y neuroblastoma cells has differential effects on the intracellular calcium concentration ([Ca2+] i) and cytotoxicity. Neurotoxicology. 2009;30(2):194–202.

39. Vilner BJ, Bowen WD. Modulation of cellular calcium by sigma-2 receptors: release from intracellular stores in human SK-N-SH neuroblastoma cells. Journal of Pharmacology and Experimental Therapeutics. 2000;292(3):900–11.

40. Akagi K, Nagao T, Urushidani T. Correlation between Ca2+ oscillation and cell proliferation via CCKB/gastrin receptor. Biochimica et Biophysica Acta (BBA)-Molecular Cell Research. 1999;1452(3):243–53.

41. Weaver EM, Zamora FJ, Hearne JL, Martin-Caraballo M. Posttranscriptional regulation of T-type Ca2+ channel expression by interleukin-6 in prostate cancer cells. Cytokine. 2015;76(2):309–20.

42. Kushner BH. Neuroblastoma: a disease requiring a multitude of imaging studies. Journal of Nuclear Medicine. 2004;45(7):1172–88.

43. Hasegawa T, Matsuzaki M, Takeda A, Kikuchi A, Akita H, Perry G, et al. Accelerated α-synuclein aggregation after differentiation of SH-SY5Y neuroblastoma cells. Brain research. 2004;1013(1):51–9.

44. Fukami K, Sekiguchi F, Yasukawa M, Asano E, Kasamatsu R, Ueda M, et al. Functional upregulation of the H2S/Cav3. 2 channel pathway accelerates secretory function in neuroendocrine-differentiated human prostate cancer cells. Biochemical pharmacology. 2015;97(3):300–9.

45. Lu F, Chen H, Zhou C, Liu S, Guo M, Chen P, et al. T-type Ca2+ channel expression in human esophageal carcinomas: a functional role in proliferation. Cell calcium. 2008;43(1):49–58.

46. Ogata N, Yoshii M, Narahashi T. Differential block of sodium and calcium channels by chlorpromazine in mouse neuroblastoma cells. The Journal of physiology. 1990;420(1):165–83.

47. C CCGUL. Molecular Operating Environment (MOE), 2019.01. Chemical Computing Group ULC 1010 Sherbooke St. West, Suite# 910, Montreal …; 2020.

48. Gaulton A, Hersey A, Nowotka M, Bento AP, Chambers J, Mendez D, et al. The ChEMBL database in 2017. Nucleic acids research. 2017;45(D1):D945–54.

49. Hall M, Frank E, Holmes G, Pfahringer B, Reutemann P, Witten IH. The WEKA data mining software: an update. ACM SIGKDD explorations newsletter. 2009;11(1):10–8.

50. Wolber G, Langer T. LigandScout: 3-D pharmacophores derived from protein-bound ligands and their use as virtual screening filters. Journal of chemical information and modeling. 2005;45(1):160–9.

51. Wishart DS, Feunang YD, Guo AC, Lo EJ, Marcu A, Grant JR, et al. DrugBank 5.0: a major update to the DrugBank database for 2018. Nucleic acids research. 2018;46(D1):D1074–82.

52. Merk D, Grisoni F, Friedrich L, Gelzinyte E, Schneider G. Computer-assisted discovery of retinoid X receptor modulating natural products and isofunctional mimetics. Journal of medicinal chemistry. 2018;61(12):5442–7.

53. Steinhardt RA, Alderton J. Intracellular free calcium rise triggers nuclear envelope breakdown in the sea urchin embryo. Nature. 1988;332(6162):364–6.

54. Chemin J, Monteil A, Briquaire C, Richard S, Perez-Reyes E, Nargeot J, et al. Overexpression of T-type calcium channels in HEK-293 cells increases intracellular calcium without affecting cellular proliferation. FEBS letters. 2000;478(1–2):166–72.

CHAPTER 07: